Cape Peninsula
University of Technology

SIMULATION OF ION EXCHANGE PROCESSES USING NEURO-FUZZY REASONING

MAGALI MARIE VAN DEN BOSCH

THESIS SUBMITTED IN FULFILMENT OF THE REQUIREMENTS FOR
THE MASTERS DEGREE IN TECHNOLOGY
(CHEMICAL ENGINEERING)

CAPE PENINSULA UNIVERSITY OF TECHNOLOGY
FEBRUARY 2009

Cape Peninsula
University of Technology

SIMULATION OF ION EXCHANGE PROCESSES USING NEURO-FUZZY REASONING

MAGALI MARIE VAN DEN BOSCH

THESIS SUBMITTED IN FULFILMENT OF THE REQUIREMENTS FOR
THE MASTERS DEGREE IN TECHNOLOGY
(CHEMICAL ENGINEERING)

SUPERVISOR: J.W. COETZEE

CAPE PENINSULA UNIVERSITY OF TECHNOLOGY
FEBRUARY 2009

DECLARATION

I certify that this report is my own unaided work, except for the assistance received from the teaching staff.

Signature..MvdBosch.....

Date.....01 February 2009.....

ABSTRACT

Neuro-fuzzy computing techniques have been approached and evaluated in areas of process control; researchers have recently begun to evaluate its potential in pattern recognition.

Multi-component ion exchange is a non-linear process, which is difficult to model and simulate as there are many factors influencing the chemical process which are not well understood. In the past, empirical isotherm equations were used but there were definite shortcomings resulting in unreliable simulations.

In this work, the use of artificial intelligence has therefore been researched to test the effectiveness in simulating ion exchange processes. The branch of artificial intelligence used was the adaptive neuro-fuzzy inference system.

The objective of this research was to develop a neuro-fuzzy software package to simulate ion exchange processes. The first step towards building this system was to collect data from laboratory scale ion exchange experiments. Different combinations of inputs (e.g. solution concentration, resin loading, impeller speed), were tested to determine whether it was necessary to monitor all available parameters. The software was developed in MS EXCEL where tools like SOLVER could be utilised whilst the code was written in Visual Basic. In order to compare the neuro-fuzzy simulations to previously used empirical methods, the Fritz and Schluender isotherm was used to model and simulate the same data.

The results have shown that both methods were adequate but the neuro-fuzzy approach was the more appropriate method.

After completion of this study, it could be concluded that a neuro-fuzzy system does not always have the ability to describe ion exchange processes adequately.

ACKNOWLEDGEMENTS

I wish to thank:

- My supervisor, Willie Coetzee for his guidance, encouragement and support;
- The staff members of the Faculty of Chemical Engineering at the Cape Peninsula University of Technology, for their encouragement and for always being willing to help;
- My parents, friends and family for their love and patience;
- Finally I would like to thank the Cape Peninsula University of Technology for their financial assistance during the period of my post-graduate studies.

TABLE OF CONTENTS

LIST OF FIGURES

LIST OF TABLES

NOMENCLATURE

Ion Exchange

A	Constant in isotherms	
A	Surface area of resin	(m^2)
B	Constant in isotherms	
C	Solution concentration	($mg.l^{-1}$)
d	Diameter	(m)
D	Surface diffusivity	($m^2.s^{-1}$)
k_f	Film diffusion coefficient	($m.s^{-1}$)
M	Mass	(g)
N	Rotational speed of impeller	(r.p.m.)
n	Constant in isotherms	
nf	Flux through the external film	
Q	Equilibrium loading	($mg.ml^{-1}$)
r	Radial variable	(m)
t	Time variable	(s)
V	Volume	(m^3)

subscripts

e	Equilibrium
p	Resin particle
R	Resin
s	liquid-adsorbent interface
0	Initial

Neural Networks

x	Input into neural network
y	Input into neural network

w	Weight in neural network
T	Variable in activation function of neural network
z	Variable in activation function of neural network
v	Variable in activation function of neural network

Neuro-fuzzy Systems

A	Fuzzy Set / Liguistic label (e.g. low, medium, high)
B	Fuzzy Set / Liguistic label (e.g. low, medium, high)
x	Input into neuro-fuzzy system
y	Input into neuro-fuzzy system
p	Consequent parameters in fourth layer of neuro-fuzzy system
q	Consequent parameters in fourth layer of neuro-fuzzy system
r	Consequent parameters in fourth layer of neuro-fuzzy system
O	Output of n^{th} layer
f	node function
μ	Membership function
a	variable in Gaussian function
c	variable in Gaussian function
w	normalised firing strength from n^{th} node

greek letters

Π	Node in second layer of neuro-fuzzy system
N	Node in third layer of neuro-fuzzy system
Σ	Node in fifth layer of neuro-fuzzy system
ρ	Density of resin ($g.m^{-3}$)

1 INTRODUCTION & LITERATURE REVIEW

1.1 HISTORICAL BACKGROUND

Up to 1850, no official studies involving ion exchange have been documented. It was not until two agricultural chemists, John Way and Harry Thompson, passed a liquid fertilizer solution containing ammonia through a soil sample, that it was discovered that the ammonia had been retained by the soil and that calcium was released into solution. Some of the observations documented formed the fundamental understanding of ion exchange:

1. The exchange of ions in soil involved the exchange of equivalent ions.
2. Some ions were more readily exchanged than others.
3. The aluminium silicates present in the soil gave it exchange characteristics.
4. The exchange of ions was different from true physical adsorption.

A few years later, the German chemist Eichorn proved that the reaction was reversible (DeSilva, 1999).

1.2 ION EXCHANGE VERSUS ADSORPTION

Sorption is a common term for adsorption and ion exchange. Most sorption technologies merely transfer the contaminant from one medium to another.

The process of adsorption involves separation of a substance from one phase accompanied by its accumulation or concentration at the surface of another.

1 INTRODUCTION & LITERATURE REVIEW

1.1 HISTORICAL BACKGROUND

Up to 1850, no official studies involving ion exchange have been documented. It was not until two agricultural chemists, John Way and Harry Thompson, passed a liquid fertilizer solution containing ammonia through a soil sample, that it was discovered that the ammonia had been retained by the soil and that calcium was released into solution. Some of the observations documented formed the fundamental understanding of ion exchange:

1. The exchange of ions in soil involved the exchange of equivalent ions.
2. Some ions were more readily exchanged than others.
3. The aluminium silicates present in the soil gave it exchange characteristics.
4. The exchange of ions was different from true physical adsorption.

A few years later, the German chemist Eichorn proved that the reaction was reversible (DeSilva, 1999).

1.2 ION EXCHANGE VERSUS ADSORPTION

Sorption is a common term for adsorption and ion exchange. Most sorption technologies merely transfer the contaminant from one medium to another.

The process of adsorption involves separation of a substance from one phase accompanied by its accumulation or concentration at the surface of another.

The molecules from the liquid or gas phase will be attached to the adsorbent in a physical manner.
An example is activated carbon, which is produced in a specific manner resulting in a large internal surface area making it ideal for the adsorption process.

Ion exchange, on the other hand, is a reversible chemical reaction involving the exchange of an ion from a liquid phase for a similarly charged ion, which is readily available from an ion exchanger, such as resin.

Ion exchange resins have been found to be more selective and durable because of their physical and chemical structure, thus serving as an ideal alternative to other recovery processes.

1.3 CONVENTIONAL MODELLING VERSUS INTELLIGENCE SYSTEMS

When building any type of simulation tool there are prominent steps to follow namely: problem identification and formulation, data collection and analysis, and Simulation Model Development (Harsham, 1990).

Problem Formulation: Identify controllable and uncontrollable inputs and constraints on the decision variables. Then define system performance and an objective function. Finally, develop a preliminary model structure to interrelate the inputs and the measure of performance.
Data Collection and Analysis: Regardless of the method used to collect the data, the decision of how much to collect is a trade-off between cost and accuracy.

Simulation Model Development: Acquiring sufficient understanding of the system to develop an appropriate conceptual, logical and then simulation model is one of the most difficult tasks in simulation analysis.

In many previous studies done with the aim of predicting ion exchange profiles, the focus was on using empirical and/or fundamental equilibrium isotherms and rate equations. This involved resistance modelling where it is assumed that equilibrium exists at the solid liquid interface and that film or intraparticle diffusion could be rate limiting.

Artificial Intelligence is a branch of science which deals with helping machines find solutions to complex problems in a more human-like fashion. This generally involves borrowing characteristics from human intelligence, and applying them as algorithms in a computer based manner. Intelligent systems adapt themselves using example situations and their correct decisions, which after the learning phase, can make decisions automatically for future situations.

1.4 ION EXCHANGE

1.4.1 Physical and Chemical Structure of Resin

Ion exchange resins are classified as cation exchangers, which have positively charged mobile ions available for exchange, and anion exchangers, where exchangeable ions are negatively charged. Both anion and cation resins are produced from the same basic organic polymers. They differ in the ionisable group attached to the hydrocarbon network. It is this functional group that determines the chemical behaviour of the resin (Remco Engineering, 1981).

The ionic groups, which are attached to the hydrocarbon network in a cation exchanger are groups such as

$-SO_3^-$, $-COO^-$, $-PO_3^{2-}$

and

$-NH_3^+$, $=NH_2^+$, $=N^+=$

for an anion exchanger.

Resins can be broadly classified as strong or weak acid cation exchangers or strong or weak base anion exchangers.

The basic requirements of resin are insolubility, bead size and resistance to fracture. Ion exchange resins can be manufactured with one of two physical structures: gel or macroporous. Gel resins are homogenous cross-linked polymers and are the most common resin available. They have exchange sites evenly distributed throughout the bead. The amount of divinylbenzene cross-linking used in the synthesis of the bead determines the strength of the structure.

Macroporous resins are manufactured by a process that leaves a network of pathways throughout the bead. This sponge-like structure allows the active part of the bead to contain a high level of divinylbenzene cross-linking without affecting the exchange kinetics. Although the macroporous resin gives a better physical stability, the gel resin has a higher operating efficiency and is less expensive.

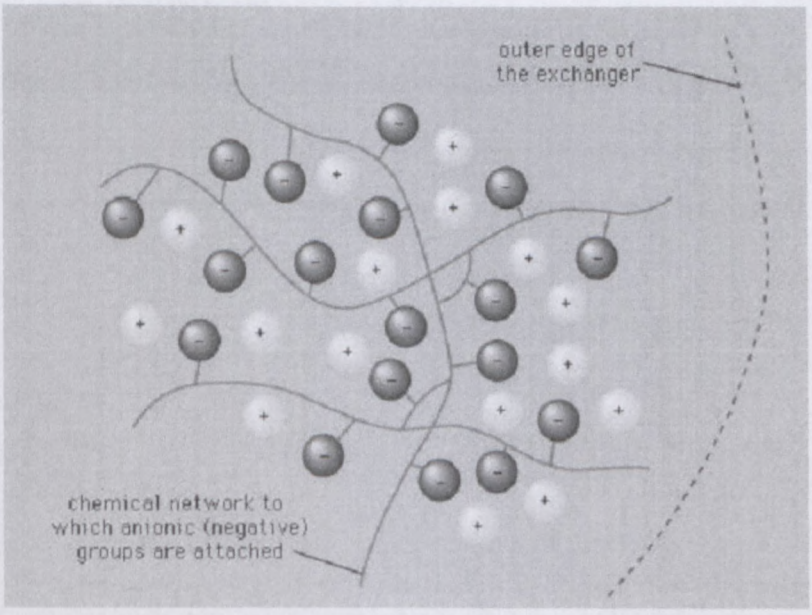

Figure 1.1: Structure of resin matrix

1.4.2 Ion Exchange Reactions

Ion exchange is a reversible chemical reaction where an ion (an atom or molecule that has lost or gained an electron and thus acquired an electrical charge) from solution is exchanged for a similarly charged ion attached to an immobile solid particle. These solid ion exchange particles are either naturally occurring inorganic zeolites or synthetically produced organic resins. The synthetic organic resins are the principal type of ion exchangers used today as their characteristics can be tailored to specific applications (Remco, 1981).

The ability to exchange ions is a result of the properties of the structure of the materials. The exchanger consists of a so-called matrix, which bears a positive or negative excess charge. This excess charge is localised in elementary cells or functional groups. As a consequence, the grid is a crystalline or high-molecular polyanion or polycation. The charge of the matrix is compensated by the so-called counter ions,

which can move within the free space of the matrix. These counter ions can be replaced by other ions of equal charge sign (Remco, 1981).

1.4.3 Mechanism of ion exchange

Ion exchange reactions are stoichiometric and reversible, and in this way are similar to other solution phase reactions. For example:

$$NiSO_4 \quad +Ca(OH)_2 \quad \leftrightarrow \quad Ni(OH)_2 \quad + \quad CaSO_4$$

In this reaction, the nickel ions of the nickel sulphate ($NiSO_4$) are exchanged for the calcium ions of the calcium hydroxide $Ca(OH)_2$ molecule. Similarly, a resin with hydrogen ions available for exchange will exchange those ions for nickel ions from solution. The reaction can be written as follows:

$$2(R\text{-}SO3H)^+ \quad NiSO_4 \quad \leftrightarrow \quad (R\text{-}SO_3)_2Ni^+ \quad H_2SO_4$$

R indicates the organic portion of the resin and SO_3 is the immobile portion of the ion active group. Two resin sites are needed for nickel ions with a plus 2 valency (Ni^{2+}).

1.4.4 Stability

During regeneration cycles, ion exchangers are subject to a variety of physical and chemical effects. These influences can cause damage for both the matrix and the functional groups.

1.4.4.1 Mechanical Stability

Mechanical damage can be caused by volume changes due to a sudden change of the resin loading. These osmotic shocks occur during regeneration when the loaded resin is contacted with the

regenerant in high concentration. Volume changes can amount to 100% of the volume of individual beads. In this respect, highly cross-linked and macroporous resins are more stable than gel-type resins. Further reasons for mechanical damage include the transport of the resin material by means of injection devices; transport in pipelines and friction during back washing in filters in fluidised beds and in valves of continually operating plants (Höll, 2004).

1.4.4.2 Thermal Stability

Thermal damage to the resin matrix is encountered if the wet resins are freezing. Therefore, resins should be stored in 10% sodium chloride solutions if there is a danger of freezing. At temperatures above the recommended values, hydrolysis affects the functional groups. Strongly acidic exchange resins gradually decompose, the functional group first breaking off followed by the degradation of the copolymer matrix. In the hydrogen form, standard resins with 8% divinylbenzene can be used at temperatures of 120 °C or more for fairly long periods. Above 150 °C, however, the resins become unstable. In the Na^+ or salt form the resins become unstable at about 180 °C. Weakly acidic ion exchangers are stable up to 75 °C whereas weakly basic exchangers can be operated up to 180 °C (Höll, 2004).

1.4.4.3 Chemical Stability

Damage due to chemical influences is mostly caused by oxidising substances. This effect is encountered in cation exchangers where the functional group cannot be oxidized further. However, anion exchangers are attacked at the functional group with a subsequent decrease of the total capacity or the conversion of strong into weak functionality (Helfferich, 1962).

1.4.5 Factors influencing equilibrium and kinetic parameters

There are various factors that may influence the kinetics of ion exchange (Helfferich, 1962):

- Movement of ions from the bulk solution
- Diffusion of ions through the laminar film surrounding the exchanger
- Diffusion of ions through the pores of the exchanger
- The physical process of ion exchange
- Diffusion of counter-ions outwards through the bead
- Diffusion of counter-ions through the laminar layer
- Movement of counter-ions into the bulk solution

It has been shown by many researchers that film and pore diffusion are the two main factors that influence the rate of ion exchange. The mathematical solution of the mass transfer equations can be achieved by either neglecting all but the rate-limiting resistances or by combining all resistances into one step (Van Deventer, 1984).

1.4.6 Rate-Controlling Steps in Ion Exchange

An intraparticle diffusion model for metal uptake kinetics is conceptualised according to the ''two-step mass transport mechanism'' (Chen et al, 2004). It is assumed that the metal ions first transfer through the external liquid film from the bulk solution, then diffuse inside the ion exchanger before being taken up by the functional group. However, the driving force for each of these two steps is different. In the liquid, the concentration difference is between the bulk solution and the liquid at the surface of the resin, which can never be larger than the bulk concentration. In the resin bead, the

concentration difference is that between the outer surface and the centre of the particle.

Although much has been documented regarding the sorption of metal ions, a comprehensive study on the rate-controlling steps has not yet been documented. However, the roles of the several relevant factors have become clear. Studies have shown that control by liquid-phase mass transfer is favoured by:

- Low liquid-phase concentration (small driving force in the liquid)
- High ion exchange capacity (large driving force in the exchanger)
- Small particle size (short mass transfer distances in the bead)
- Open structure of the exchanger, e.g. low cross-linking (little obstruction to diffusion in the exchanger)
- Ineffective agitation of the liquid (low contribution to convection to liquid-phase mass transfer) (DeSilva, 1999).

With regard to diffusion it can be imagined that ion exchange depends on the wandering of ions within the solution, across the boundary film around the resin particle and within the resin bead to and from the exchange site. Some of these effects are probably the controlling factors of the process. However, it has been found that the exchange rate may obey neither model equations for diffusion, whether it is film or particle, nor chemically controlled mechanisms (Ling et al, 2004).

1.4.7 Equilibrium Expressions

Equilibrium studies are used to evaluate the sorbate sorption capacity. Batch kinetic studies are employed to investigate the mass transfer properties of the adsorbent (Chen, 2004). Sorption can be expressed by an ion exchange isotherm where the concentration of a counter-ion in the ion exchanger is expressed as a function of its concentration in the external solution under specified conditions and at constant temperature.

Common single solute sorption isotherms used are:

Linear isotherm:

$$q_e = AC_e \tag{1.1}$$

which is only applicable at very low equilibrium concentration where no interaction takes place between adsorbed species.

Freundlich isotherm (Freundlich, 1926):

$$q_e = AC_e^n \tag{1.2}$$

which is widely used to describe single solute sorption but does not approach true linearity at low equilibrium concentration.

Langmuir isotherm (Zeng et al, 1995):

$$q_e = \frac{AC_e}{B + C_e} \tag{1.3}$$

which is widely used at low concentrations.

The single component Freundlich and Langmuir isotherms may both be extended to incorporate other adsorbing species to account for a multi-component system.

Multi-component Freundlich isotherm:

$$q_{e,i} = A_i C_{e,i}\left[C_{e,i} + \sum_{j=1}^{N} B_{i-j} C_{e,j} \right]^{ni-1} \qquad (1.4)$$

Multi-component Langmuir isotherm:

$$q_{e,i} = \frac{A_i C_{e,i}}{1 + \sum_{j=1}^{N} A_j C_{e,j}} \qquad (1.5)$$

Fritz and Schluender (1974) suggested a general empirical equation for calculating the adsorption equilibrium of components in aqueous solutions.

$$q_{e,i} = \frac{A_i C_{e,i}^{\ ni}}{D_i + \sum_{j=1}^{N} A_j C_{e,j}^{\ nj}} \qquad (1.6)$$

As a result of its flexibility, this type of isotherm was used in this study.

1.4.8 Sorption kinetics

For the purpose of this project it is assumed that film diffusion is the rate-limiting factor. This assumption is defended by the macroporous structure of the resin.

It is further assumed that the rate of mass transfer through the liquid film is concentration gradient dependent; hence Fick's first law may be used:

$$n_f = -D\frac{\partial C}{\partial r} \tag{1.7}$$

Hence,

$$n_f = k_f(C - C_s) \tag{1.8}$$

where $k_f = \frac{D}{\sigma}$ (2.9)

A mass balance over a batch reactor yields:

$$-V\frac{dC}{dt} = \mathrm{n}_f A \tag{1.10}$$

Assuming that all the resin particles are spherical and equal in size, the surface area is calculated by:

$$A = \frac{6M}{\rho_R d_p} \tag{1.11}$$

Substituting equations (1.8) and (1.11) into equation (1.8) the following is obtained:

$$-V\frac{dC}{dt} = \mathrm{n}_f\frac{6M}{\rho_R d_p} = \frac{k_f(C - C_s)6M}{\rho_R d_p} \tag{1.12}$$

The liquid phase material balance in a batch reactor yields:

$$\frac{dC}{dt} = \frac{6k_f M}{\rho_R d_p V}(C_s - C) \tag{2.13}$$

The value of C_s is obtained by employing a suitable equilibrium isotherm as it is assumed that equilibrium exists at the solid liquid interface.

Assuming that the concentration at the solid liquid interface is negligible compared to the bulk liquid concentration in the early stages, equation 2.13 becomes:

$$\frac{dC}{dt} = \frac{6k_f M}{\rho_R d_p V} C \qquad (1.14)$$

The film transfer coefficient is determined by integrating equation 1.14, yielding:

$$\ln\left(\frac{C_o}{C}\right) = \frac{6k_f M}{\rho_R d_p V} t \qquad t \rightarrow 0 \qquad (1.15)$$

A plot of $ln(C_0/C)$ over time for the initial stages of the ion exchange process can be used to obtain the value of k_f.

It must be emphasised that this type of diffusion technique is by no means novel and that similar reasoning has been used in the past (Van Deventer, 1984).

1.5 NEURO-FUZZY SYSTEMS

Most processes in industry are characterised by their non-linear and time-varying behaviour, which makes non-linear system identification an important tool when mathematically modelling these types of applications. Neuro-fuzzy modelling can be regarded as grey box techniques as it involves the use of physical laws and observed measurements when applied to designing a model. Neuro–fuzzy systems combine the semantic transparency of rule-based fuzzy systems with the learning capability of neural networks (Jang et al, 1997).

A very good understanding of both neural-networks and rule-based fuzzy systems is essential as it forms the backbone of neuro-fuzzy systems. Both neural-networks and fuzzy systems are motivated by imitating human reasoning processes.

1.5.1 Fuzzy Models

A mathematical model, which in some way uses fuzzy sets, is called a fuzzy model. Fuzzy systems are general approximators, capable of accurately representing non-linear processes and including existent knowledge about a process (Pedrycz et al, 1997).

In system identification, rule-based fuzzy models are usually applied. In these models, the relationships between variables are represented by means of 'if–then' rules with imprecise (ambiguous) predicates, such as:

If heating is high then temperature increase is fast.

This rule defines, in a rather qualitative way, the relationship between the heating and the temperature in a room. To make such a model operational, the meaning of the terms 'high' and 'fast' must be defined more precisely. This is done by using fuzzy sets, i.e. sets where the membership changes gradually rather than in an abrupt way. Fuzzy sets are defined through their membership functions, which map the elements of the considered universe to the unit interval [0; 1]. The extreme values 0 and 1 denote complete membership and non-membership, respectively, while a degree between 0 and 1 means partial membership in the fuzzy set. Depending on the structure of the if–then rules, two main types of fuzzy models can be distinguished: the

Mamdani (or linguistic) model and the Sugeno Fuzzy model (Babuška, 2003).

1.5.1.1 Mamdani Fuzzy Model

In this model, the antecedent (if-part of the rule) and the consequent (then-part of the rule) are fuzzy propositions:

R: If x is *A* then *y* is *B*,

Here *A* and *B* are the antecedent and consequent linguistic terms (such as 'small', 'large', etc.), represented by fuzzy sets. The linguistic fuzzy model is useful for representing qualitative knowledge. The Mamdani model is typically used in knowledge-based (expert) systems.

1.5.1.2 Sugeno Fuzzy Model

In data-driven identification, this type of model proposed by Takagi and Sugeno (1985) in an effort to develop a systematic approach to generating fuzzy rules from a given input-output data set, has become popular.. A typical fuzzy rule of the Sugeno fuzzy model has the form:

R: If x is *A* and *y* is *B* then $z = f(x,y)$,

where *A* and *B* are fuzzy sets in the antecedent, while $z = f(x,y)$ is a crisp function in the consequent. Usually $f(x,y)$ is a polynomial in the input variables x and *y*, but it can be any function as long as it approximates the output.

1.5.2 Artificial Neural Networks

Artificial neural networks (ANNs), originally inspired by the functionality of biological neural networks, can learn complex functional relations by generalising from a limited amount of training data. ANNs can thus serve as black-box models of non-linear, multivariable static and dynamic systems and can be trained by using input–output data observed. The most common ANNs consist of several layers of simple processing elements called neurons, interconnections among them and weights assigned to these interconnections. The information relevant to the input–output mapping of the net is stored in the weights.

1.5.2.1 Multi-Layer Neural Network

A feed forward multi-layer neural network (MNN) has one input layer, one output layer and any number of hidden layers between them. The input-layer neurons do not perform any computations; they merely distribute the inputs x_i to the weights w_{ij}^h of the hidden layer. In the neurons of the hidden layer, the weighted sum of the inputs is computed

$$z_j = \sum_{i=1}^{p} w_{ij}^h x_i = (w_j^h)^T x, \qquad j = 1,2,\ldots,m \tag{1.16}$$

It is then passed through a non-linear activation function, such as the tangent hyperbolic:

$$v_j = \frac{1-\exp(-2z_j)}{1+\exp(-2z_j)} \qquad j = 1,2,\ldots,m \tag{1.17}$$

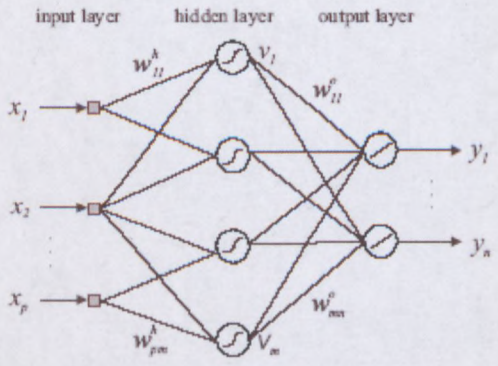

Figure 1.2 A feedforward neural network with one hidden layer (Babuška, 2003)

Other typical activation functions are the threshold function (hard limiter) and the sigmoid function. The neurons in the output layer are linear, i.e., only the weighted sum of their inputs are computed:

$$y_l = \sum_{j=1}^{n} w_{jl}^{o} v_j = (w_l^o)^T x \qquad l = 1,2,\ldots\ldots,n \qquad (1.18)$$

Training is the adaptation of weights in a multi-layer network such that the error between the desired output and the network output is minimised. Two steps are distinguished in this procedure:

1. *Feed forward computation.* From the network inputs x_i, the outputs of the first hidden layer are first computed. Then using these values as inputs to the second hidden layer, the outputs of the next layer are computed, etc. Finally, the output of the network is obtained.

2. *Weight adaptation.* The output of the network is compared to the desired output. The difference of these two values, the error, is then used to adjust the weights first in the output layer, then in the layer before, etc., in order to decrease the error (gradient-descent optimisation). This backward computation is called 'error back propagation' (Babuška, 2003).

A network with one hidden layer is sufficient for most approximation tasks. More layers can give a better result, but the training takes longer. Choosing the correct number of neurons in the hidden layer is essential for a good result. Too few neurons give a poor fit, while too many neurons result in over training of the network (poor generalisation to unseen data). A compromise is usually sought by trial and error.

1.5.3 Neuro-Fuzzy Modelling

Presently, the neuro-fuzzy approach is becoming one of the major areas of interest as a result of the benefits of combining neural networks and fuzzy logic systems. First approaches were mainly concentrated on neuro-fuzzy controllers whereas newer approaches can now also be found in data analysis. Nauck (1995) concluded that the neuro-fuzzy approach went beyond simple control applications.

Neural networks and fuzzy logic have some common features such as distributed representation of knowledge, model-free estimation and ability to handle data with uncertainty and imprecision. Fuzzy logic has tolerance for imprecision of data, while neural networks have tolerance for noisy data. In order to identify a suitable fuzzy system for a given problem, membership functions (parameters) and a rule base (structure) must be specified. This can be done by prior knowledge, by learning, or by a combination of both. If a learning algorithm is applied that uses local information and causes local modifications in a fuzzy system, the approach is usually called a neuro-fuzzy system (Nauck et al, 1999).

Neuro-fuzzy modelling refers to the manner of applying various learning techniques developed in the neural network literature to fuzzy modelling or to a fuzzy inference system (FIS). The basic structure of a FIS consists of three conceptual components: a rule base, which contains a selection of fuzzy rules; a database which defines the membership functions (MF) used in the fuzzy rules; and a reasoning mechanism, which performs the inference procedure upon the rules to derive an output (Nayak et al, 2004).

Both prior knowledge and process data can be used to construct a neuro-fuzzy system; expert knowledge is formulated as a collection of if-then rules. In this way an initial model is created. The parameters in the model (membership function, consequent and modifiable parameters) are then fine-tuned by using process data (Babuška, 2003).

A well-known neuro-fuzzy system used for function approximation is ANFIS (adaptive neuro-fuzzy inference system), and will be applied in order to reach the objective of simulating ion exchange profiles.

1.5.3.1 Architecture of ANFIS

There are two basic steps to system identification: structure identification and parameter estimation. The choice of structure is a very important aspect as it determines the flexibility of the model in the approximation system. A model with a rich structure can approximate more complicated functions but at the same time worsen generalisation properties. Good generalisation means that a model fitted to one data set will perform well on another data set of the same process.

ANFIS is a class of adaptive networks that are functionally equivalent to fuzzy inference systems (Jang, 1993). For simplicity, a two input fuzzy inference system is described.

Consider a first-order Sugeno fuzzy model with the following two fuzzy if-then rules:

Rule 1: If x is A_1 and y is B_1 then, $f_1=p_1x + q_1y+r_1$

Rule 2: If x is A_2 and y is B_2 then, $f_1=p_2x + q_2y+r_2$

Figures 2.3 and 2.4 illustrate the reasoning mechanism for the Sugeno model as well as the corresponding equivalent ANFIS structure, where the nodes of the same layer have similar functions. (The output of the i^{th} node in layer *l* is denoted as $O_{l,i}$).

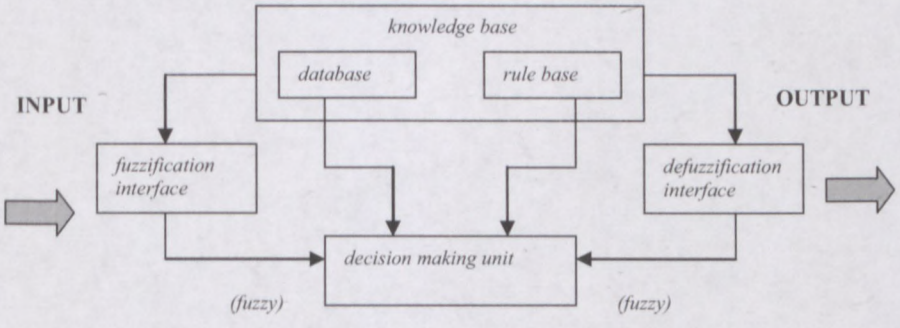

Figure 1.3: Fuzzy Inference System with crisp output. (Nayak et al, 2004)

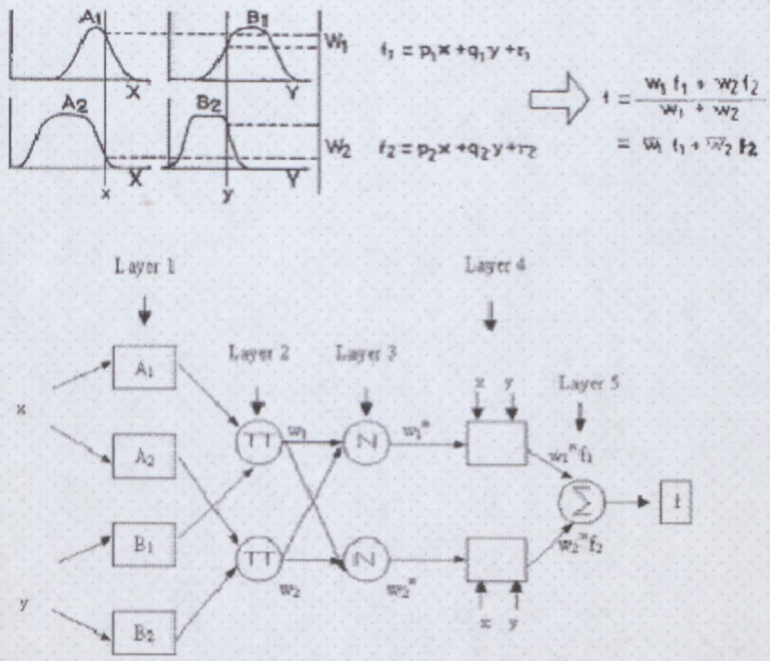

Figure 1.4: (a) Fuzzy inference system. (b) Equivalent ANFIS architecture. (Jang et al, 1997)

Layer 1: Every node in this layer is an adaptive node with a node function

$$O_{1,i} = \mu A_i(x), \qquad \text{for } i = 1, 2 \tag{1.19}$$

$$O_{1,i} = \mu B_i(y) \tag{1.20}$$

where x (or y) is the input to node *i* and A_i (or B_i) is a linguistic label (such as "low" or "high") associated with this node. In other words, $O_{1,i}$ is the membership grade of a fuzzy set A and it specifies the degree to which the given input x (or y) satisfies the quantifier A. Here the membership function for A can be any appropriate parameterised membership such as the bell function or the Gaussian function:

$$\mu_A(x) = \exp\left[-\frac{(x-c_i)^2}{2a_i^2}\right] \tag{1.21}$$

where *a* and *c* are the modifiable parameters. As the values of these parameters change, the function varies accordingly, thus exhibiting various forms of membership function for fuzzy sets. Parameters in this layer are referred to as premise parameters.

Layer 2: Each node in this layer labelled Π is fixed, their outputs are the product of the all the incoming signals:

$$O_{2,i} = w_i = \mu_{A_i}(x)\mu_{B_i}(y), \quad i = 1,2 \tag{1.22}$$

Each node output represents the firing strength of a rule.

Layer 3: Each node in this layer labelled *N* is fixed; the i^{th} node calculates the ratio of the i^{th} rule's firing strength to the sum of all rules firing strengths:

$$O_{3,i} = \overline{w_i} = \frac{w_i}{w_1 + w_2}, \quad i = 1,2 \tag{1.23}$$

For convenience, the outputs in this layer are referred to as normalised firing strengths.

Layer 4: Each node I in this layer is an adaptive node with a node function

$$O_{4,i} = \overline{w_i} f_i = \overline{w_i}(p_i x + q_i y + r_i) \tag{1.24}$$

where w_i is a normalised firing strength from layer 3 and $\{p_i, q_i, r_i\}$ is the parameter set of this node. Parameters in this layer are referred as consequent parameters.

Layer 5: The single fixed node in this layer labelled Σ, computes the overall output as the summation of all incoming signals:

$$overall\_output = O_{5,1} = \sum \overline{w_i} f_i = \frac{\sum_i w_i f_i}{\sum_i w_i} \tag{1.25}$$

This adaptive network is functionally equivalent to a Sugeno fuzzy model. The choice of the model's structure is very important as it determines the flexibility of the model in the approximation of systems. In neuro-fuzzy models, the architecture of the structure involves the selection of input variables as well as the number and types of membership functions and the number of rules.

The input variables give insight in the process behaviour and are a source of information for the choice of initial sets and possible inputs. The type of membership functions and number of rules are two structural parameters, which are related and determine the level of detail (granularity) of the model (Babuška, 2003).

1.5.3.2 Structure and Parameter Learning

Any designed simulation system has to be linked to an optimisation technique to be used effectively for systems design. In a function approximation problem, plain supervised learning may be used as a result of knowledge obtained from input and output vectors (fixed learning problem). This means that if suitable rules for certain areas are known, the neuro-fuzzy system can be initialised. The remaining rules have to be found by learning (Nauck et al, 1997). It results in shifting the membership functions, and in making their supports larger or smaller, eventually optimising the system.

Several learning algorithms or tools are available for training fuzzy systems, but will not be discussed in detail, as optimisation algorithms are not the focus of this study. The tool used to train the system and determine the values for the premise parameters and the consequent parameters in this study is a Newtonian search method built into MS EXCEL. This technique will be verified using MATLAB ANFIS Toolbox.

1.6 OBJECTIVES AND METHODOLOGY OF THIS STUDY

Although much research has been done on ion exchange and intelligence systems individually, little has been done to use AI techniques in predicting ion exchange profiles. It was decided to launch an investigation where the classical method of profile prediction is compared with a neuro-fuzzy approach. The following steps were followed:

- Batch experiments were performed involving multi-component ion exchange in order to develop a comprehensive database containing ion exchange kinetic values with corresponding resin loadings, solution concentrations, pH and agitation rates.
- Using the above-mentioned data, a multi-component isotherm was developed in order to predict the ion exchange process with a classical method.
- A Visual Basic programme, capable of evaluating the effectiveness of a neuro-fuzzy approach to ion exchange using the sum of error squared criteria between actual data and simulation results, was developed.
- Neuro-fuzzy simulated results were compared to those obtained from classical dual resistance modelling in order to establish whether the proposed technique is indeed more suitable than frequently used methods.

2 EXPERIMENTAL AND DATA BASE GENERATION

As mentioned previously, the selection of inputs to neuro-fuzzy systems is a critical aspect of modelling. The database was generated by collecting a large number of data points from ion exchange experimental data.

2.1 Materials and Experimental Set-up

AMBERJET 1200H, a strong acid cation resin produced by Rohm & Haas, was used as an ion exchanger. This exchanger is used industrially for demineralisation. Copper- and cobalt sulphate of an analytical grade dissolved in deionised water was used as sorbing ions.

2.1.1 Regeneration of resin

Before performing the experiments, the resin had to be treated to make sure it was in the sodium form. This was done by first passing a solution of hydrochloric acid through a column filled with resin until the pH of the effluent was equal to that of the influent. The resin was washed with deionised water to remove excess ions. Sodium hydroxide was then passed through the column to convert the resin to the sodium form. This continued until the pH of the effluent was equal to the influent and then washed again with deionised water.

Figure 2.1: Regeneration of resin

2.1.2 *Two-Component Ion Exchange Experiments*

A batch configuration consisting of a one-litre flask and an overhead stirrer set at speeds of 120, 200 and 300 rpm was employed. A flat blade impeller was used for agitation.

Ten ml resin was added to the solution and samples were taken with a syringe at different intervals for a period of two hours. All samples were then diluted and analysed with an Atomic Absorption Spectrometer (AA). The amount of metal ions taken up by the resin was determined by doing a mass balance over the system.

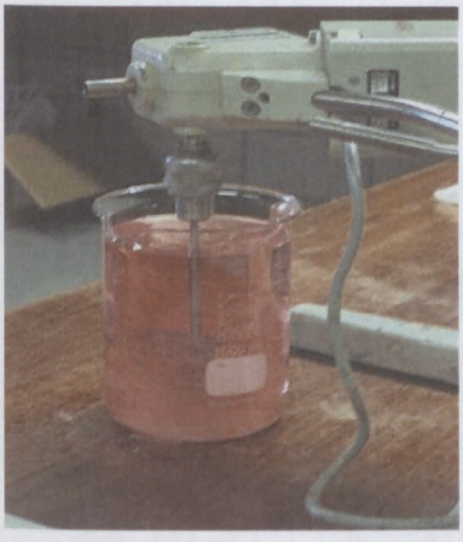

Figure 2.2: Experimental Set-up

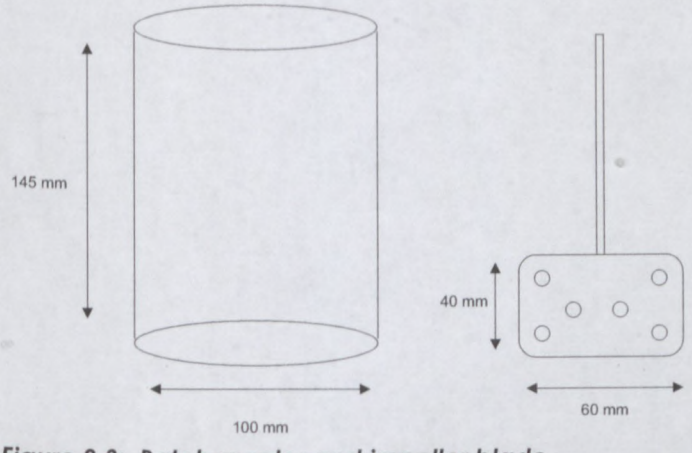

Figure 2.3: Batch reactor and impeller blade

Table 2.1: Experiments performed

Experiment	Copper Concentration (mg/l)	Cobalt Concentration (mg/l)	Stirring Speed (rpm)
1	500	500	120
2	500	1000	120
3	500	1500	120
4	1000	500	120
5	1000	1000	120
6	1000	1500	120
7	1500	500	120
8	1500	1000	120
9	1500	1500	120
10	500	500	200
11	500	1000	200
12	500	1500	200
13	1000	500	200
14	1000	1000	200
15	1000	1500	200
16	1500	500	200
17	1500	1000	200
18	1500	1500	300
19	500	500	300
20	500	1000	300
21	500	1500	300
22	1000	500	300
23	1000	1000	300
24	1000	1500	300
25	1500	500	300
26	1500	1000	300
27	1500	1500	300

2.1.3 *Verification of results*

An experimental overall mass balance over the reactor was performed to verify the accuracy of the method of calculating resin loading. After completing an experiment, the resin was taken out of the solution and stripped with sulphuric acid. The remaining solution was then analysed for copper and cobalt, which resulted in 98.9 % accuracy. It was assumed that all the copper and cobalt were removed from the resin and that the imperfect accuracy was due to experimental error.

2.2 Generation of database

Ten data points were collected from each experiment at different intervals. Trend lines were fitted to these points in order to generate a sufficient number of input/output combinations. A typical ion exchange reaction can be divided into three stages; the first stage is where the rate of change in concentration is linear with time; a second stage where the rate of change in concentration diminishes at increased rate and the third stage where equilibrium is reached. The first stage trend line is merely a linear plot whereas the second and third stages were combined with a third order polynomial fit. By employing the trend line, numerous data points could be generated by simple differentiation.

3 METHODOLOGY

3.1 Classical Modelling

Assuming that mass transfer is film transport controlled, a film diffusion model as shown in equation 1.13 can be employed. The solution concentration at the liquid-adsorbent interface (C_s) can be obtained from equation 1.6, assuming that the Fritz & Schluender isotherm accurately describes equilibrium conditions for the multi component system.

Using equation 1.15, the film diffusion coefficients were calculated for both copper and cobalt. This was done by linearising equation 1.14 and plotting $ln(C_0/C)$ versus time, from which the slope A equal to $\frac{6k_f M}{\rho_R d_p V}$ can be determined.

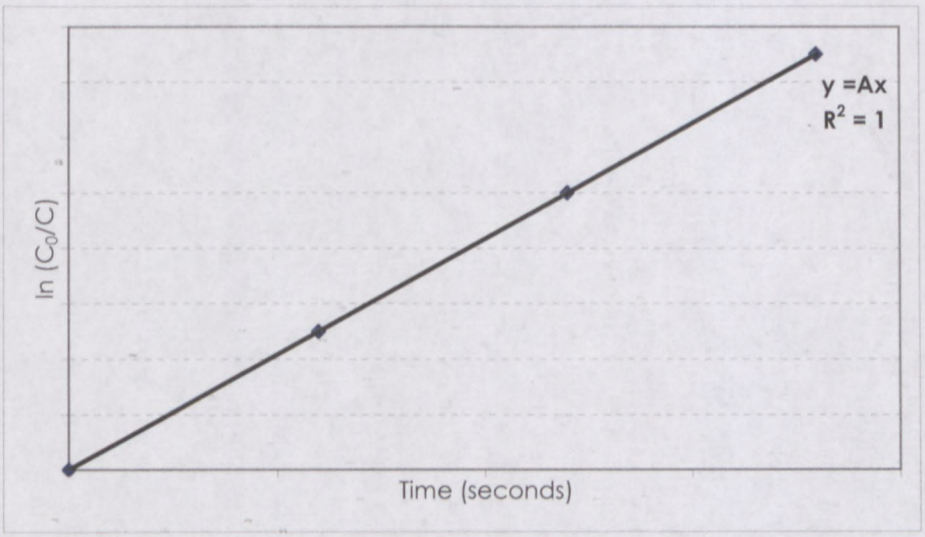

Figure 3.1: Linearisation of Film Diffusion Model

As a number of variables had to be solved simultaneously in the Fritz and Schluender isotherm, SOLVER was used to find the optimum

solution by applying the sum of squares of error criteria. The selection of the various starting points was of utmost importance as SOLVER has difficulties in solving variables if the initial values are out of range.

3.2 Neuro-Fuzzy System

As mentioned in the previous section, a database is critical when modelling a neuro-fuzzy system. After evaluating all the experimental results, the following inputs and outputs were available:

Inputs:

- Concentration of copper in solution
- Concentration of cobalt in solution
- Loading of copper on the resin
- Loading of cobalt on the resin
- Total metal loading on the resin
- Stirring speed

Outputs:

- Change in concentration of copper
- Change in concentration of cobalt

The programme written in Visual Basic was developed so that it could take up to five inputs and one output. The MS EXCEL sheet as indicated below contains the database and the "start" button. The "start" button activates a user interface for specifying inputs and outputs.

V	W	X	Y	Z	AA	AB	AC
[Cu]	q(Cu)	dCu/dt	[Co]	q(Co)	dCo/dt	q(Tot)	N
474.5	0	-0.93713	531	0	-1.568191	0	120
463.3758	1.589173	-0.91516	512.4928	2.643888	-1.511182	4.233061	120
452.5124	3.141089	-0.893705	494.6819	5.188294	-1.452081	8.329383	120
441.9036	4.656622	-0.872753	477.5887	7.630179	-1.391555	12.2868	120
431.5436	6.136623	-0.85229	461.2271	9.967557	-1.330174	16.10418	120
421.4265	7.581922	-0.832303	445.6044	12.19937	-1.268449	19.78129	120
411.5468	8.				-1.206839	23.31872	120
401.8989	10.				-1.145751	26.71776	120
392.4779	11.				-1.085542	29.9803	120
383.2792	13.				-1.026521	33.10877	120
374.2986	14.				-0.968951	36.10601	120
365.5327	15.				-0.91305	38.97516	120
356.979	16.				-0.858994	41.7196	120
348.6359	17.98059	-0.685774	346.4643	26.36225	-0.806922	44.34283	120
340.503	19.14243	-0.668229	337.0582	27.70596	-0.756936	46.84839	120
332.5814	20.27409	-0.650537	328.2402	28.96568	-0.709107	49.23977	120
324.8734	21.37523	-0.632568	319.9841	30.14513	-0.663478	51.52035	120
317.3832	22.44526	-0.614189	312.2633	31.24809	-0.620068	53.69335	120
310.1164	23.48337	-0.595263	305.0513	32.27839	-0.578872	55.76175	120
303.0803	24.48852	-0.575659	298.3215	33.23978	-0.539868	57.7283	120
296.2838	25.45946	-0.555262	292.0479	34.13602	-0.50302	59.59548	120
289.7368	26.39474	-0.533975	286.2048	34.97074	-0.468278	61.36549	120

START

Figure 3.2: Start Button and database

When starting the programme, a form will appear as shown below where the inputs and output can be specified:

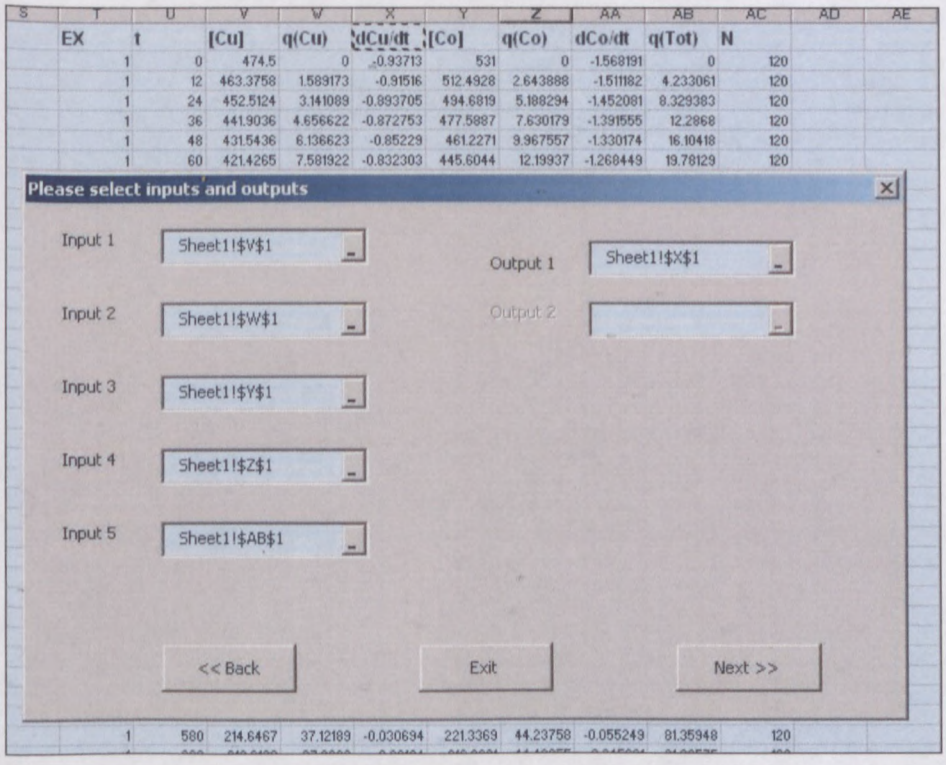

Figure 3.3: Selections of Inputs and Outputs

The programme will then automatically take the next cell below the heading and read in the data until the first empty cell is reached. Pressing the next button will call SOLVER. All of the steps, which occur to model the system, can be summarized as follows:

1. The Gaussian and consequent parameters (*c, a, p, q, r, s, t*) as discussed in the literature section are initialised.
2. The three values from the low, medium and high Gaussian functions are then calculated.

$$\mu_A(x) = \exp\left[-\frac{(x-c_i)^2}{2a_i^2}\right] \tag{3.1}$$

3. The low Gaussian functions for each input are multiplied by each other, resulting in a weight value for the low. This procedure is repeated for the medium and high Gaussian function.

$$O_{2,i} = w_i = \mu_{A_i}(x)\mu_{B_i}(y), \tag{3.2}$$

4. These three weights are then divided by the sum of the three weights to calculate the weighted weight.

$$O_{3,i} = \overline{w_i} = \frac{w_i}{w_1 + w_2} \tag{3.3}$$

5. The contribution from each weight towards the output is then calculated.

$$O_{4,i} = \overline{w_i} f_i = \overline{w_i}(p_i x + q_i y + r_i) \tag{3.4}$$

6. The total sum of the three contributions is then calculated to determine the overall output.

$$overall\_output = O_{5,1} = \sum \overline{w_i} f_i = \frac{\sum_i w_i f_i}{\sum_i w_i} \qquad (3.5)$$

7. The sum of differences between the actual and the calculated outputs are determined.
8. The model will be trained using SOLVER, which will then adjust the modifiable and consequent parameters to decrease the sum of the differences of the outputs and return to Step 1.The above steps will be repeated until the smallest possible sum of differences is reached.
9. The modelling process is now completed and the programme will automatically draw a graph showing the actual and calculated output. An R^2 value is also displayed below the graph. This is an indication of how a change in the input will relate to the output. The final parameters are also saved in MS EXCEL format, which will be used in the future to simulate ion exchange profiles.

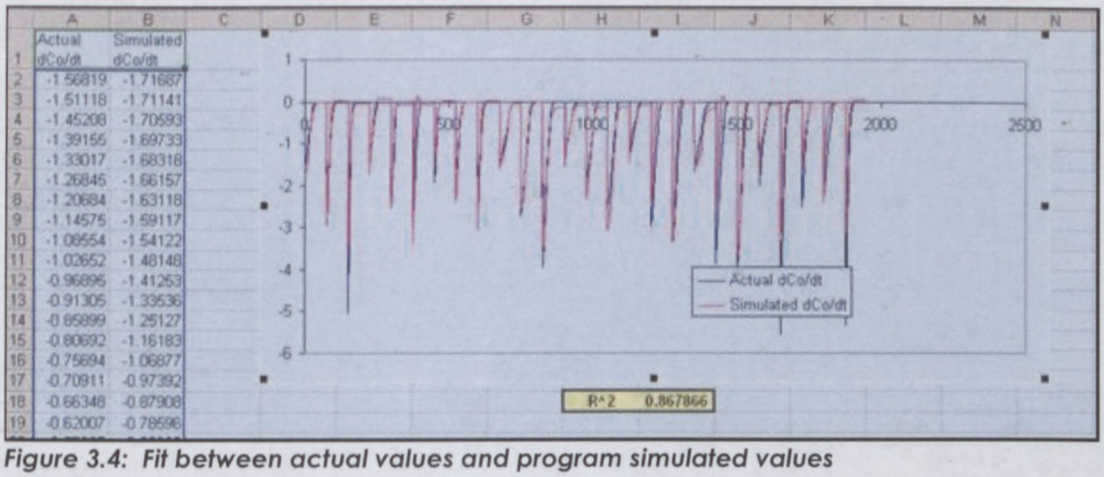

	Actual dCo/dt	Simulated dCo/dt
2	-1.56819	-1.71687
3	-1.51118	-1.71141
4	-1.45208	-1.70593
5	-1.39155	-1.69733
6	-1.33017	-1.68318
7	-1.26845	-1.66157
8	-1.20684	-1.63118
9	-1.14575	-1.59117
10	-1.08554	-1.54122
11	-1.02652	-1.48148
12	-0.96895	-1.41253
13	-0.91305	-1.33536
14	-0.85899	-1.25127
15	-0.80692	-1.16183
16	-0.75694	-1.06877
17	-0.70911	-0.97392
18	-0.66348	-0.87908
19	-0.62007	-0.78596

Figure 3.4: Fit between actual values and program simulated values

3.2.1 Optimisation/Training Technique

SOLVER

The SOLVER option in MS EXCEL may be used to solve linear and non-linear optimisation problems. It can be retrieved in the Tools menu in MS EXCEL. Integer restrictions may be placed on the decision variables. SOLVER may be used to solve problems with up to 200 decision variables, 100 explicit constraints and 400 simple constraints (lower and upper bounds and/or integer restrictions on the decision variables). Decision variables can also be constrained with respect to each other e.g.: A>B).

SOLVER uses the Generalized Reduced Gradient Algorithm for optimising non-linear problems. SOLVER uses iterative numerical methods that involve "plugging in" trial values for the adjustable cells and observing the results calculated by the constraint cells and the optimum cell. Each trial is called an iteration. As a pure "trial and error" approach would take an extremely long time (especially for problems involving many adjustable cells and constraints), SOLVER performs extensive analyses of the observed outputs and their rates of change as the inputs are varied, to guide the selection of new trial values.

In a typical problem, the constraints and the optimum cell are functions of (that is, they depend on) the adjustable cells. The first derivative of a function measures its rate of change as the input is varied. When there are several values entered, the function has several partial derivatives measuring its rate of change with respect to each of the input values; together, the partial derivatives form a vector called the gradient of the function (Microsoft Knowledge Base Article – 82890).

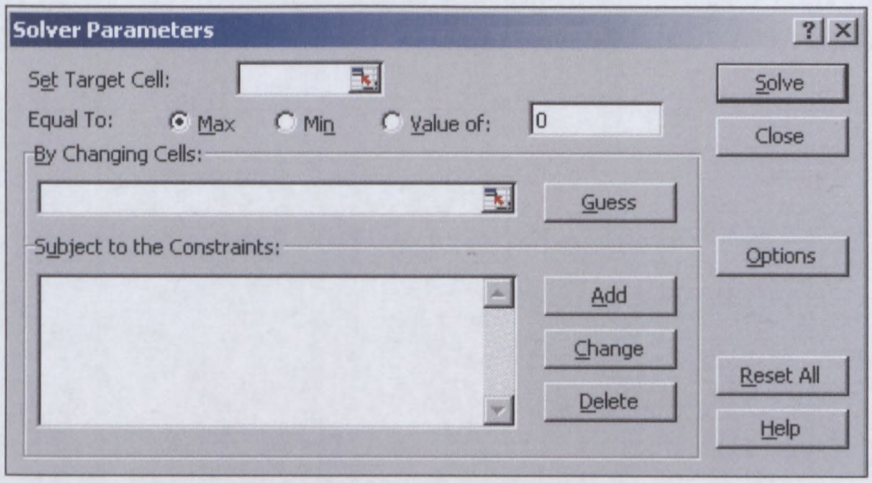

Figure 3.5: SOLVER parameter dialog box

The **Set Target Cell** box should contain the cell location of the objective function for the problem under consideration. Error or parameter to be maximised, minimized or set equal to a specific value.

Max or **Min** may be selected for finding the maximum or minimum of the set target cell. If **Value** is selected, the SOLVER will attempt to find a value of the Target Cell equal to whatever value is placed in the box just to the right of this selection.

The **By Changing Cells** box should contain the location of the parameters to be manipulated for the problem.

Finally, the constraints must be specified in the **Subject to the Constraints** box by clicking on Add.

Example:

Suppose an equation needs to be solved with four different variables. Let us assume that it is known that the answer "a" must be 10 and it has

to be solved for the other three unknown variables "x, y and z".

$a = \sin(x) + \cos(y) + \tan(y/z)$

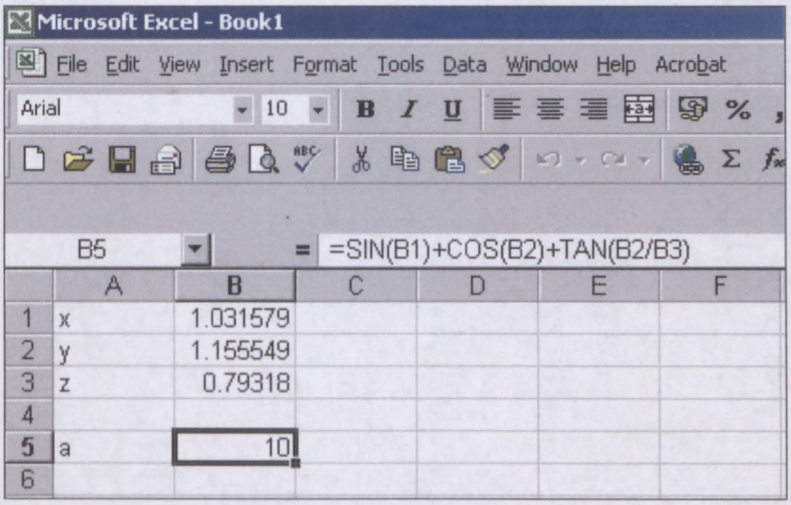

Figure 3.6: A simple MS EXCEL procedure

With this problem, certain constraints were given:

$a = 10;\ x > 1\ ;\ y > 0.5;\ z < 15$

To solve for the unknown variables the following steps are used:

1. Select Tools and then SOLVER.
2. Click on the Set Target Cell box and type B5.
3. Click on Value.
4. Click on the By Changing Cells box and, in the spreadsheet, click and drag mouse from B1 to B3.
5. Click the Add button to invoke the Add Constraint dialogue box.
6. To enter the constraints: Click in the Cell Reference box and enter B1 to B3 in the Cell Reference box as well as each variable's constraint. Click on Add.
7. Click Solve.

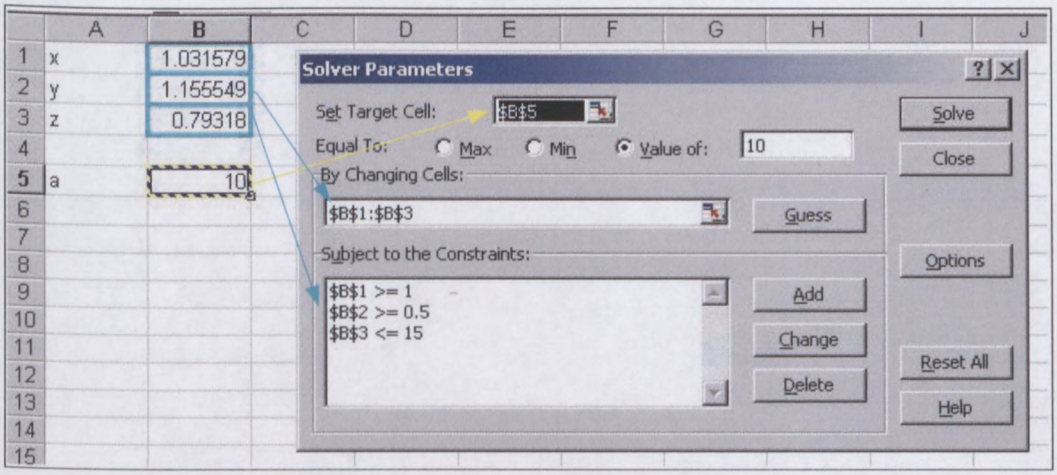

Figure 3.7: Application of SOLVER on a simple MS EXCEL procedure

A macro can be run from the Visual Basic interface in MS EXCEL, which can reproduce the same procedure without having to use the SOLVER dialogue box.

```
Sub Macro_Solver()
    SolverOk SetCell:="$B$5", MaxMinVal:=3, ValueOf:="10", ByChange:="$B$1:$B$3"
    SolverAdd CellRef:="$B$1", Relation:=3, FormulaText:="1"
    SolverOk SetCell:="$B$5", MaxMinVal:=3, ValueOf:="10", ByChange:="$B$1:$B$3"
    SolverAdd CellRef:="$B$2", Relation:=3, FormulaText:="0.5"
    SolverAdd CellRef:="$B$3", Relation:=1, FormulaText:="10"
    SolverOk SetCell:="$B$5", MaxMinVal:=3, ValueOf:="10", ByChange:="$B$1:$B$3"
    SolverDelete CellRef:="$B$3", Relation:=1, FormulaText:="10"
    SolverAdd CellRef:="$B$3", Relation:=1, FormulaText:="15"
    SolverOk SetCell:="$B$5", MaxMinVal:=3, ValueOf:="10", ByChange:="$B$1:$B$3"
    SolverSolve
End Sub
```

Figure 3.8: Macro running SOLVER from VBA

When using a macro, it has to be ensured that SOLVER.xla has been loaded as a reference in VBA. As mentioned in the previous section, SOLVER was used to adjust the Gaussian and consequent parameters.

Three different methods of solving were used:

SOLVER 1 minimises the output error by first changing the Gaussian parameter; then, after reaching a minimum error, the consequent parameters are modified to produce a lower error.

SOLVER 2 was equivalent to the SOLVER 1, but one step was added. After having solved for the Gaussian and consequent parameters individually, the minimising of the sum of the errors of outputs was repeated but this time by solving for both the Gaussian and consequent parameters at once, therefore using initial parameters much closer to the optimum value.

SOLVER 3 was done solving for both the Gaussian and consequent parameters by minimising the sum of the errors of the outputs all at once. This last approach had to be ruled out, as reasonable error could not be obtained.

The R-square value is an indicator of how well changes in the output parameters are explained by changes in the input variables.

The lowest error was reached when the input subset of characteristics is composed of concentration of copper, concentration of cobalt, loading of copper on resin, loading of cobalt on resin and stirring speed.

The SOLVER 3 ANFIS models were omitted as the R square values reached were below 0.4.

4 FRITZ & SCHLUENDER ISOTHERM AND FILM DIFFUSION MODEL SIMULATIONS

The isothermal experiments were conducted under different conditions. It was concluded that the Fritz and Schluender isotherm provided reasonable equilibrium estimates. The Fritz and Schluender parameters are given in equations 4.1 and 4.2. In order to find the kinetic controlling mechanisms, experiments at three different stirring speeds were conducted. The kinetic model data is summarised in Table 4.1. With an increase in the stirring speed, k_f values increased.

Using the initial concentrations of an experiment, linearising these values and plotting them over time, the slope yielded a value from which the diffusion coefficient was determined.

Time (sec)	Cu Conc (mg/l)	ln(C0/C) Cu
0	1000.0	0.00
150	758.3	0.28
300	606.1	0.50
450	600.9	0.51
600	593.2	0.52
900	527.1	0.64
1200	591.9	0.52
1800	602.0	0.51
3600	608.8	0.50
7200	612.5	0.49

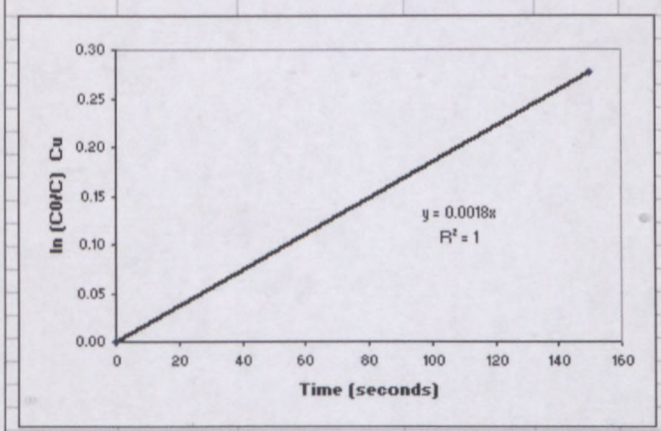

Figure 4.1: Determining film diffusion coefficients from slope

From equation 1.15 the slope is equal to $\frac{6k_f M}{\rho_R d_p V}$, therefore one can determine the k_f values using the following equation:

$$k_f = \frac{slope * d_p * V}{6 * V_{resub}}$$

$$k_f = \frac{0.0018 * 0.630 * 1}{6 * 7} = 0.000027 \text{ m.s}^{-1}$$

After doing this for each experiment, an average was taken for each stirring speed.

Table 4.1: Film diffusion coefficient of each metal at different stirring speeds

rpm		k_f (m/s)
120	Cu	0.00001952
120	Co	0.00003974
200	Cu	0.00003173
200	Co	0.00004119
300	Cu	0.00003337
300	Co	0.00004724

The estimation of the variables of the Fritz & Schluender isotherm was done by giving these unknown variables guessed but realistic initial values, thereafter an ion exchange profile was determined using these values.

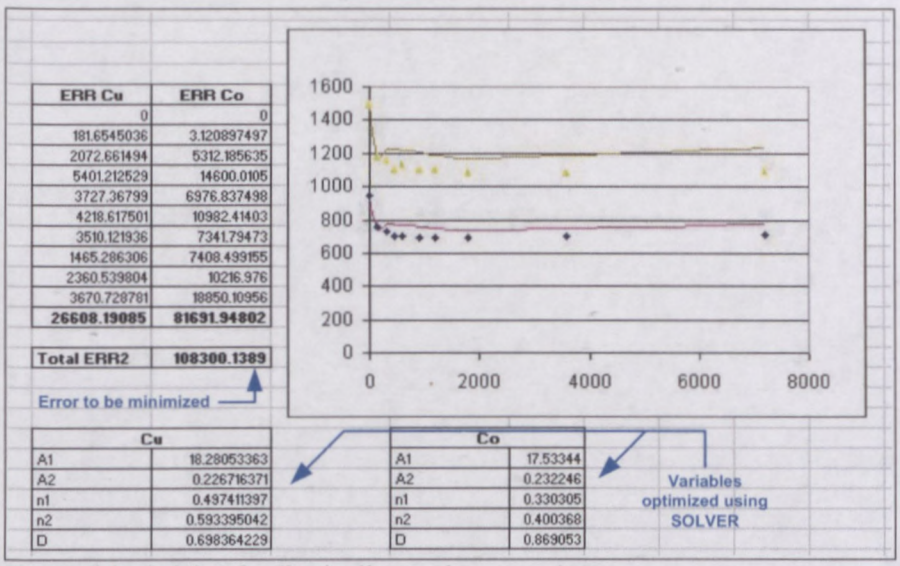

Figure 4.2: Solving for the isothermal parameters

An error was calculated between the simulated and actual concentrations for both copper and cobalt; then SOLVER was used to minimise the error of the sum of the two errors by changing the isothermal parameters so that the simulated and actual concentration were as close to each as possible. The following equations were determined for both copper and cobalt.

$$q_{Cu} = \frac{18.281 C_{Cu}^{\ 0.497}}{0.698 + 0.227 C_{Co}^{\ 0.593}} \qquad (4.1)$$

$$q_{Co} = \frac{17.533 C_{Co}^{\ 0.33}}{0.869 + 0.232 C_{Cu}^{\ 0.4}} \qquad (4.2)$$

The mass transfer and equilibrium parameters obtained above were in the classical simulation approach. The model predictions are shown in Figures 4.3 to 4.5, indicating a relatively good model fit.

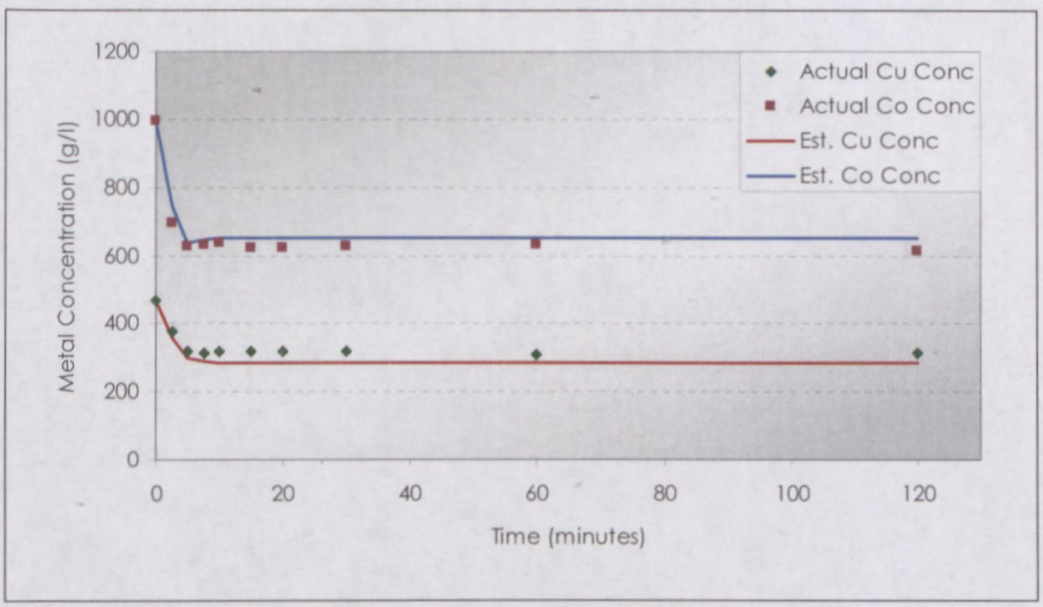

Figure 4.3: Film Diffusion - The sorption of 500 mg/l copper and 1000 mg/l cobalt onto 10 ml of resin at 120 rpm

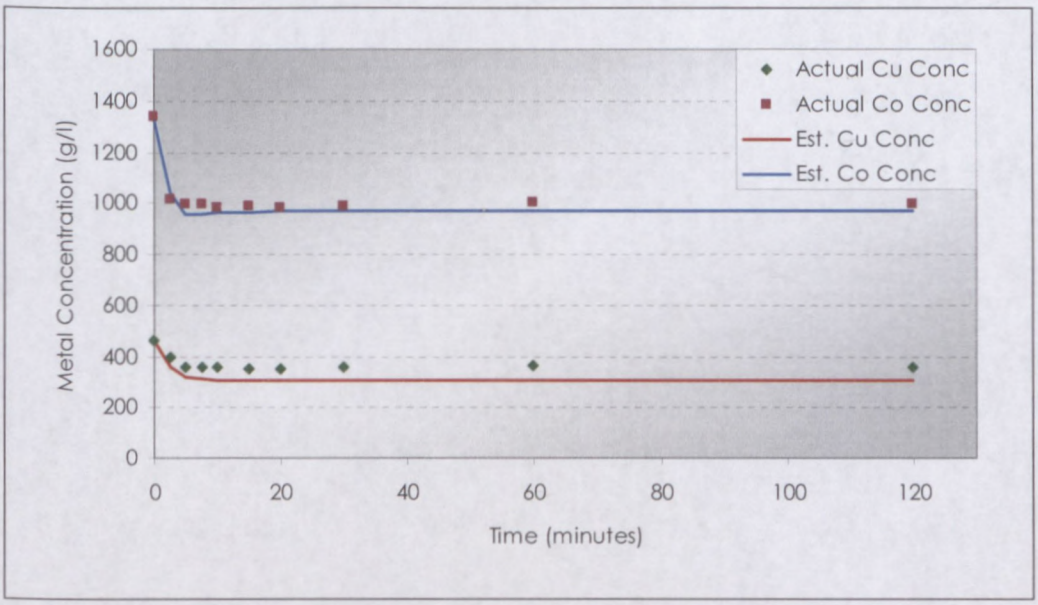

Figure 4.4: Film Diffusion - The sorption of 500 mg/l copper and 1500 mg/l cobalt onto 10 ml of resin at 200 rpm

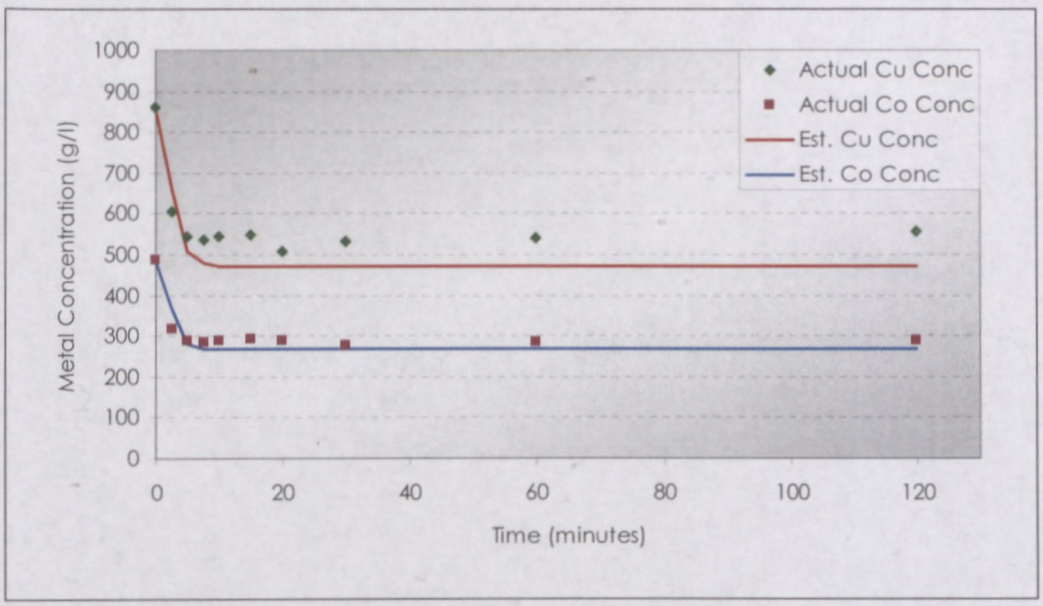

Figure 4.5: Film Diffusion - The sorption of 1000 mg/l copper and 500 mg/l cobalt onto 10 ml of resin at 300 rpm

5 ANFIS MODEL SIMULATIONS

The learning rule of ANFIS training is a hybrid learning which combines the gradient descent and the least squares method for an effective search of optimal parameters. The neuro-fuzzy systems had 30 to 42 adjustable parameters, which had to be solved. The number of adjustable parameters depended on the chosen number of rules and inputs. The parameter learning was constrained so that the membership functions maximums do not "cross".

Before the training commenced, a selection method appropriate for the ANFIS structure was carried out to determine if the proposed features were relevant, or if any subset of them would produce better results.

An analysis considering possible combinations of 1, 2, 3, 4, 5 and 6 inputs were conducted obtaining the minimum error of the ANFIS structure set after training. The first column in Table 5.1 indicates the number of inputs used and the second column shows the combination of these inputs resulting in a minimum error.

Table 5.1: Different Models Constructed

Model	Method of training	Number of Characteristics / Inputs	Inputs *
ANFIS 1	SOLVER 1	3	1,2,3
ANFIS 2	SOLVER 2	3	1,2,3
ANFIS 3	SOLVER 1	4	1,2,3,6
ANFIS 4	SOLVER 2	4	1,2,3,6
ANFIS 5	SOLVER 1	5	1,2,4,5,6
ANFIS 6	SOLVER 2	5	1,2,4,5,6
ANFIS 7	SOLVER 1	5	1,2,3,4,5
ANFIS 8	SOLVER 2	5	1,2,3,4,5

* 1 Concentration of copper, 2: Concentration of cobalt, 3: Loading of copper on the resin, 4: Loading of cobalt on the resin, 5: Total metal loading on the resin, 6: Stirring speed:

Neuro-fuzzy systems to model for three, four and five inputs and one output were structured. As each model could only incorporate one output, it had to be run twice to determine the change in concentration of both copper and cobalt.

5.1 ANFIS 1 & 2: Model with 3 Inputs

The first system was structured by selecting three inputs and feeding them to the network. The selection of the inputs was based on the assumptions that the chemical reaction was irreversible, and as the resin took up copper and cobalt ions, the loading would not be affected by the free counter-ions which had come off the resin (Na^+).
It was also assumed that the individual loading of each component did not have an effect on the rate of sorption and is only affected by the total metal loading. Stirring speed was not included in this model.

SOLVER 1

ANFIS 1: Model with 3 Inputs

Inputs:	
Concentration of copper	
Concentration of cobalt	
Total metal loading on resin	
Outputs:	**R^2**
Change in concentration of copper	**0.715**
Change in concentration of cobalt	**0.832**

SOLVER 2

ANFIS 2: Model with 3 Inputs

Inputs:	
Concentration of copper	
Concentration of cobalt	
Total metal loading on resin	
Outputs:	**R^2**
Change in concentration of copper	**0.749**
Change in concentration of cobalt	**0.832**

The simulations from ANFIS 1 gave appropriate results at the higher stirring speed whereas for the low stirring speed, there was a definite deviation from the experimental data.

ANFIS 2, which is equivalent to ANFIS 1, varying only in the training approach, was more successful even though the same amount of data was fed to the system. This shows that extensive training has a positive effect. Although the R square values of both ANFIS 1 and 2 were very similar, it resulted in a better simulation.

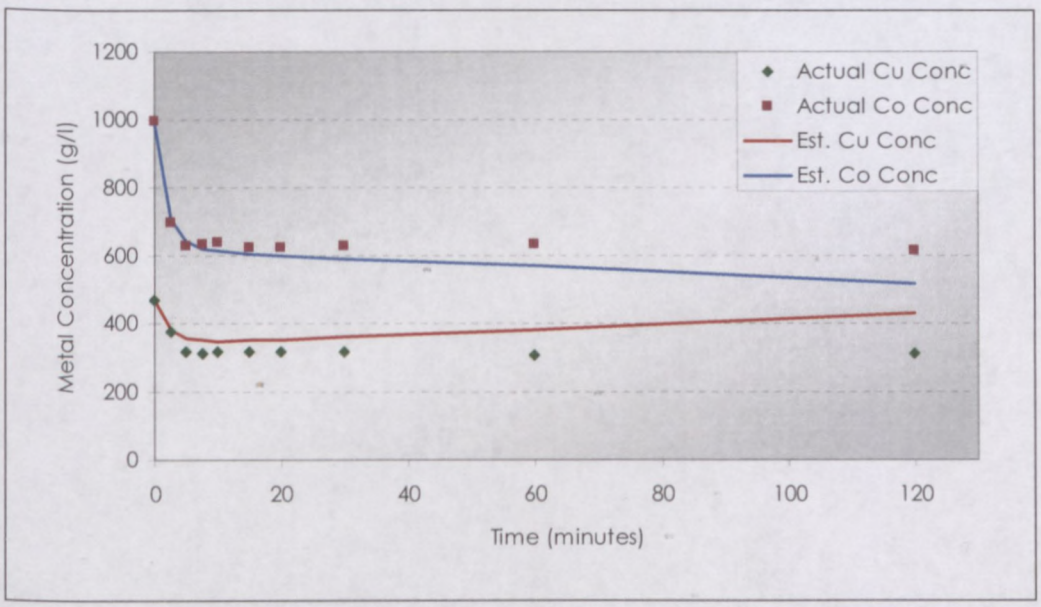

Figure 5.1: ANFIS 1 - The sorption of 500 mg/l copper and 1000 mg/l cobalt onto 10 ml of resin at 120 rpm

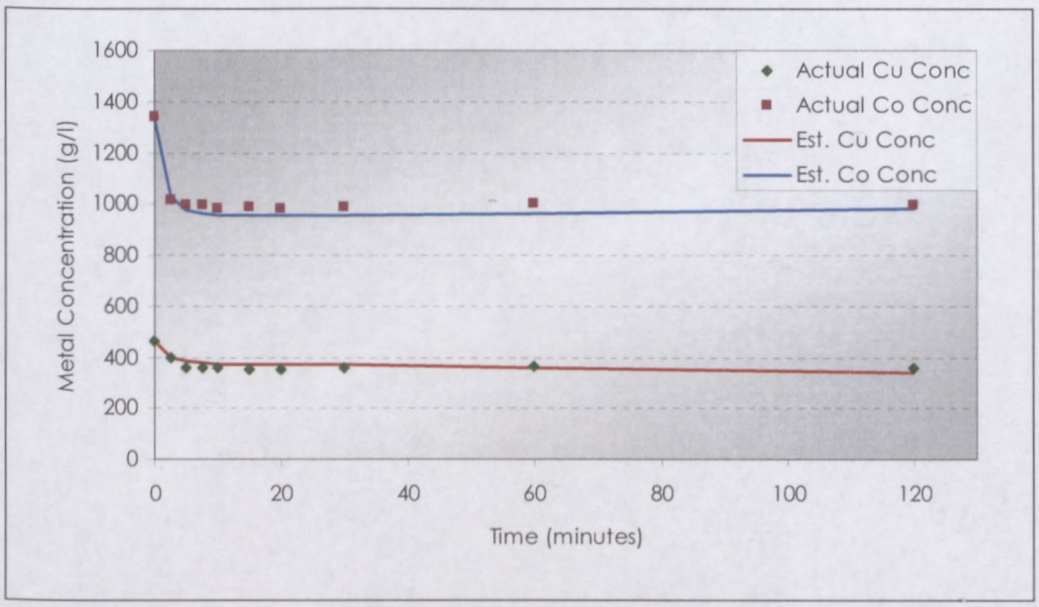

Figure 5.2: ANFIS 1 - The sorption of 500 mg/l copper and 1500 mg/l cobalt onto 10 ml of resin at 200 rpm

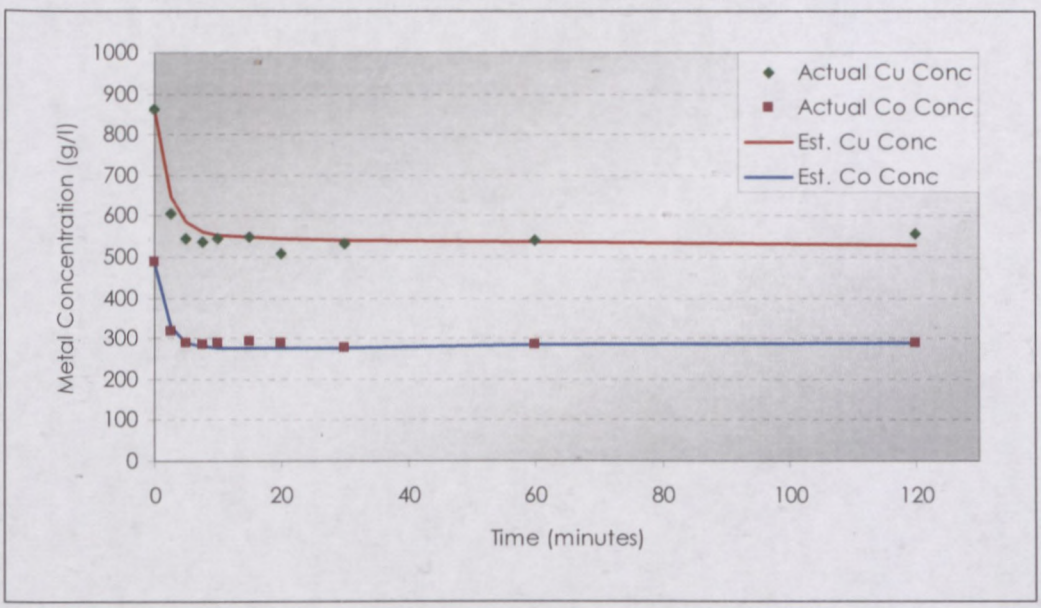

Figure 5.3: ANFIS 1 - The sorption of 1000 mg/l copper and 500 mg/l cobalt onto 10 ml of resin at 300 rpm

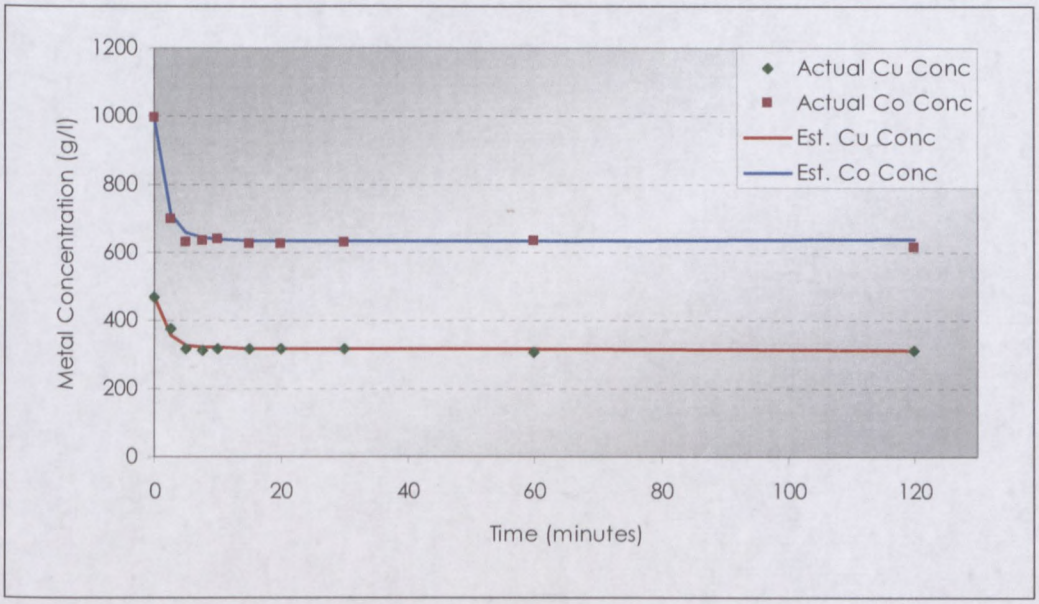

Figure 5.4: ANFIS 2 - The sorption of 500 mg/l copper and 1000 mg/l cobalt onto 10 ml of resin at 120 rpm

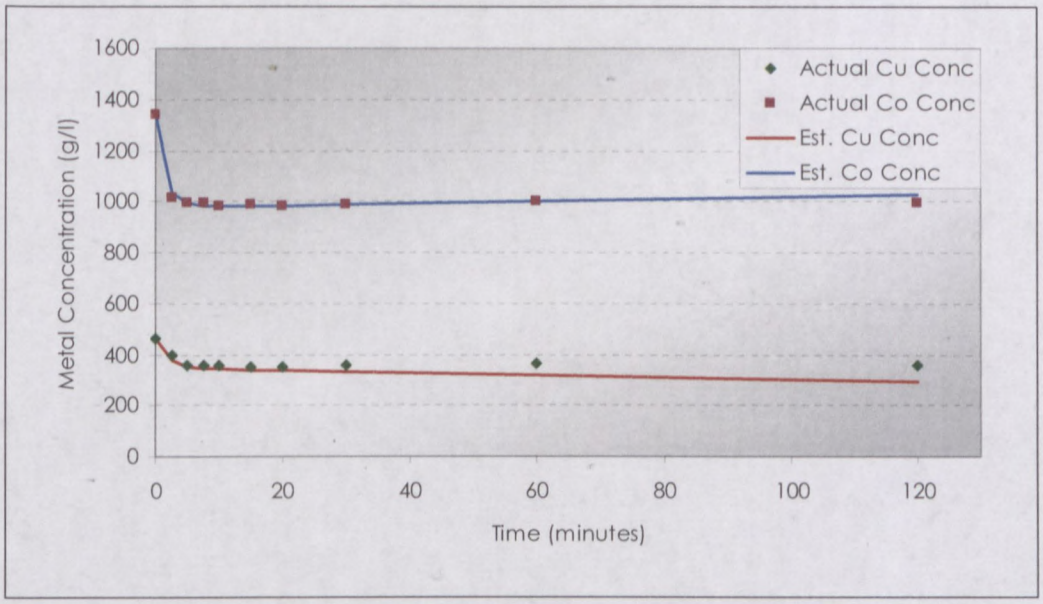

Figure 5.5: ANFIS 2 - The sorption of 500 mg/l copper and 1500 mg/l cobalt onto 10 ml of resin at 200 rpm

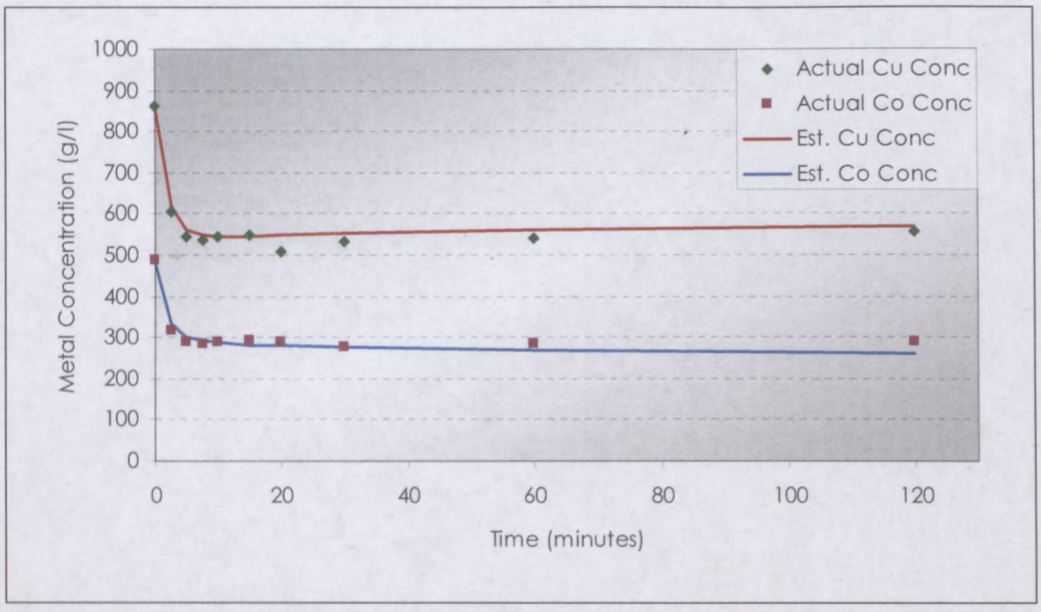

Figure 5.6: ANFIS 2 - The sorption of 1000 mg/l copper and 500 mg/l cobalt onto 10 ml of resin at 300 rpm

5.2 ANFIS 3 & 4: Model with 4 Inputs

Similarly to the ANFIS 1 & 2, the concentrations of copper and cobalt, as well as the total loading on the resin were used, with the only difference being that the stirring speed was incorporated.

SOLVER 1

ANFIS 3: Model with 4 Inputs

Inputs:	
Concentration of copper	
Concentration of cobalt	
Total metal loading on resin	
Stirring Speed	
Outputs:	**R^2**
Change in concentration of copper	**0.674**
Change in concentration of cobalt	**0.839**

SOLVER 2

ANFIS 4: Model with 4 Inputs

Inputs:	
Concentration of copper	
Concentration of cobalt	
Total metal loading on resin	
Stirring Speed	
Outputs:	**R^2**
Change in concentration of copper	**0.754**
Change in concentration of cobalt	**0.893**

The inclusion of the stirring speed in ANFIS 3 seemed to have a negative effect on the R squared value of the copper but a positive effect on cobalt although when ANFIS 4 was further trained, there was a significant increase in the value of the R square for both copper and cobalt. Even though there was a decrease in the R square value of ANFIS 3, the simulations, which were generated for cobalt, were more successful than the ANFIS 1 up to equilibrium where the copper started to go off-track. This was the case for ANFIS 4 as well but less significantly. Overall the simulations did not show a definite increase in accuracy when the stirring speed was incorporated.

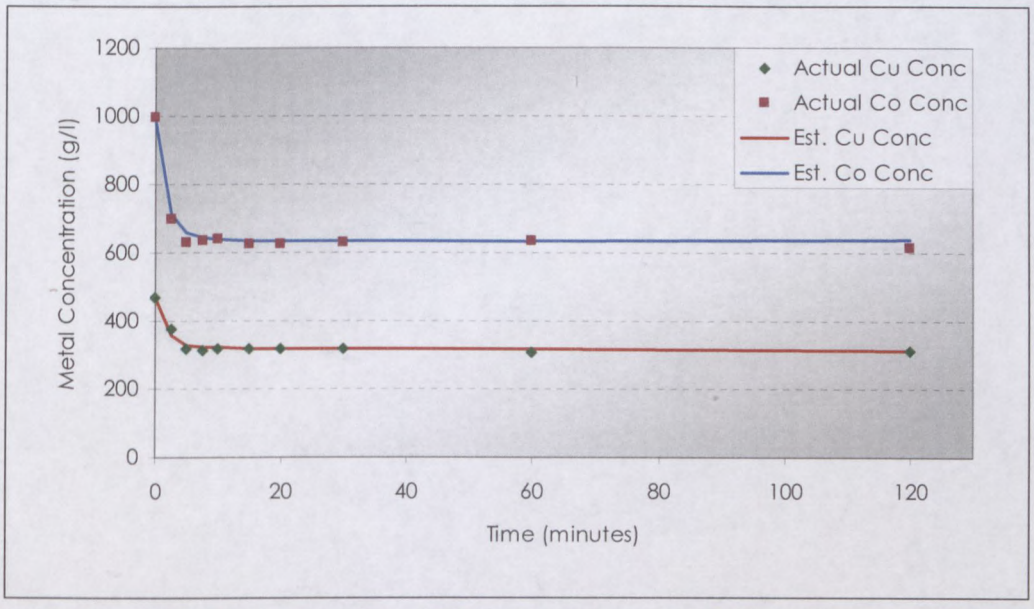

Figure 5.7: ANFIS 3 - The sorption of 500 mg/l copper and 1000 mg/l cobalt onto 10 ml of resin at 120 rpm

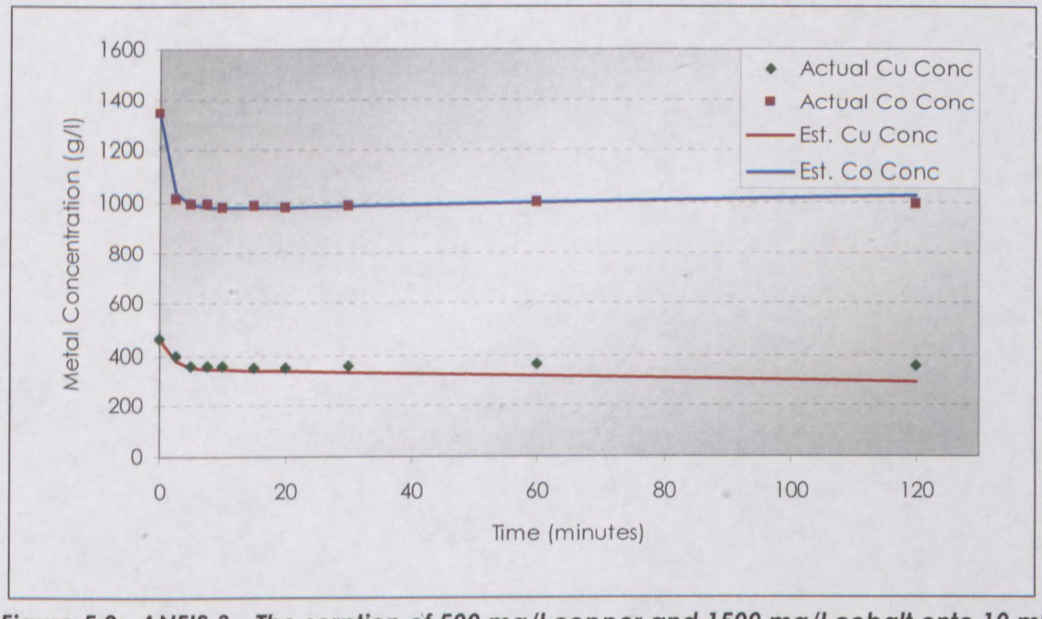

Figure 5.8: ANFIS 3 - The sorption of 500 mg/l copper and 1500 mg/l cobalt onto 10 ml of resin at 200 rpm

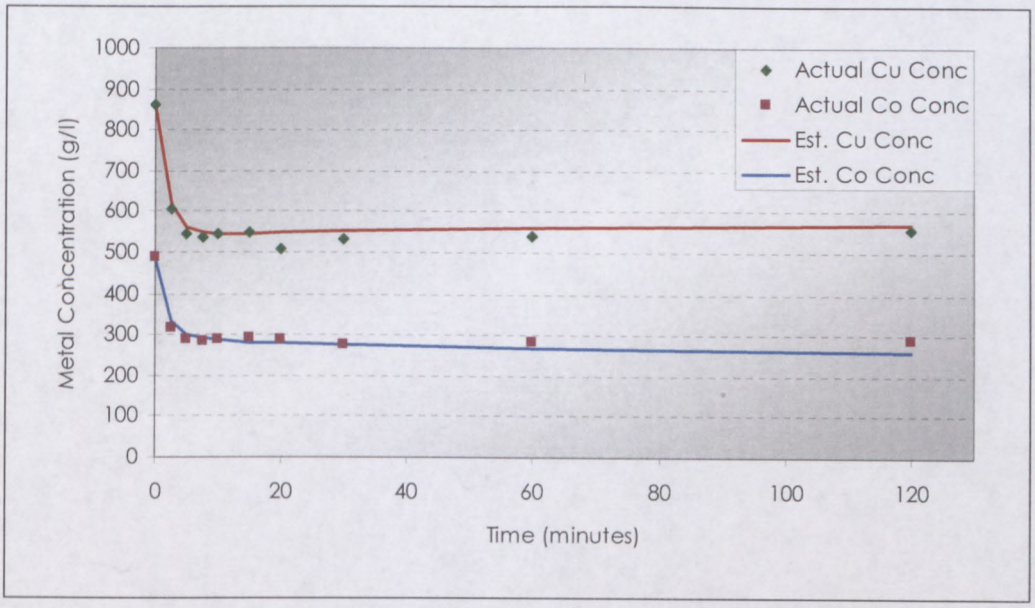

Figure 5.9: ANFIS 3 - The sorption of 1000 mg/l copper and 500 mg/l cobalt onto 10 ml of resin at 300 rpm

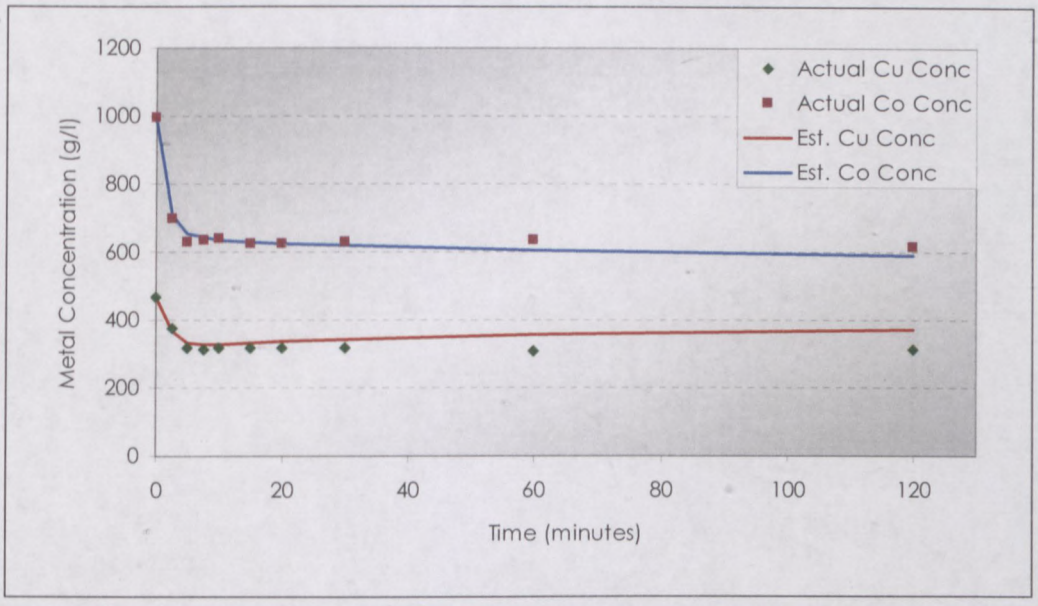

Figure 5.10: ANFIS 4 - The sorption of 500 mg/l copper and 1000 mg/l cobalt onto 10 ml of resin at 120 rpm

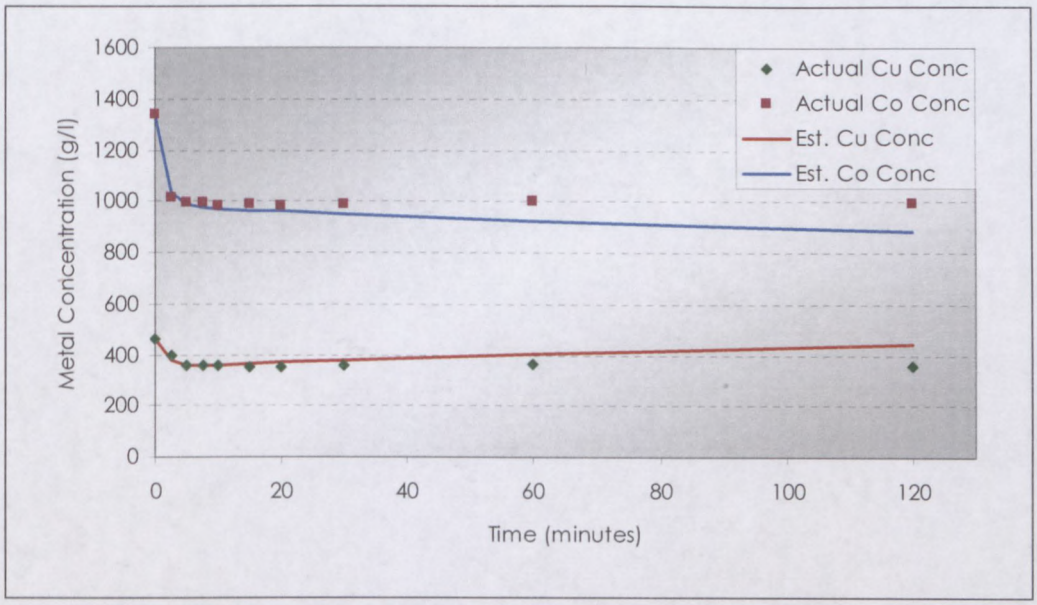

Figure 5.11: ANFIS 4 - The sorption of 500 mg/l copper and 1500 mg/l cobalt onto 10 ml of resin at 200 rpm

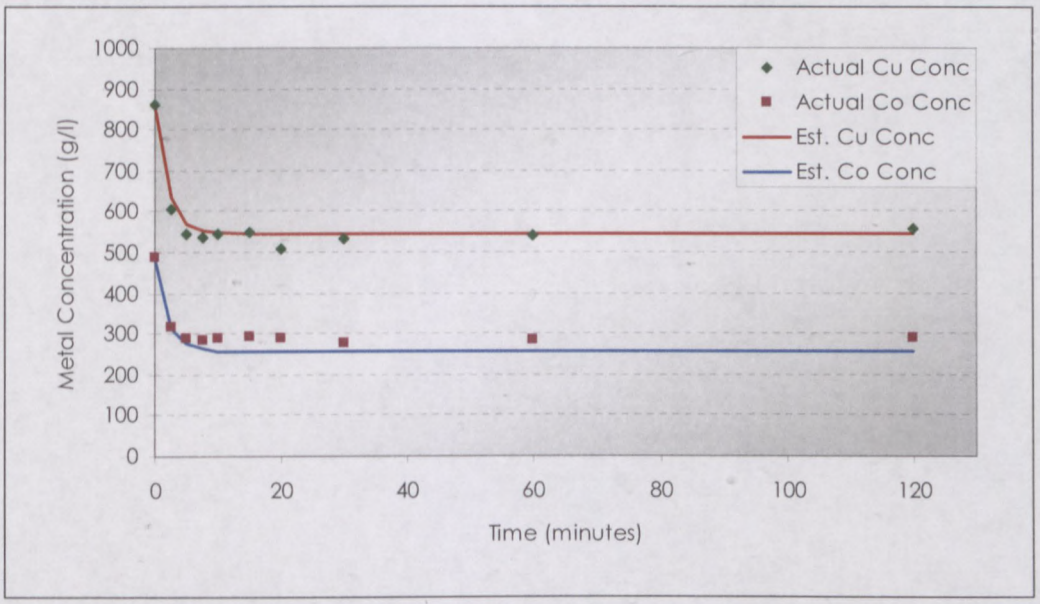

Figure 5.12: ANFIS 4 - The sorption of 1000 mg/l copper and 500 mg/l cobalt onto 10 ml of resin at 300 rpm

5.3 ANFIS 5 & 6: Model with 5 Inputs

Similar to ANFIS 3 & 4, this model incorporated the two metal concentrations and stirring speed. Also, a distinction was made between the specific loading of each metal on the resin. This inclusion of individual loadings was expected to lead to more accurate simulation results.

SOLVER 1

ANFIS 5: Model with 5 Inputs

Inputs:	
Concentration of copper	
Concentration of cobalt	
Loading of copper on resin	
Loading of cobalt on resin	
Stirring Speed	
Outputs:	**R^2**
Change in concentration of copper	**0.712**
Change in concentration of cobalt	**0.886**

SOLVER 2

ANFIS 6: Model with 5 Inputs

Inputs:	
Concentration of copper	
Concentration of cobalt	
Loading of copper on resin	
Loading of cobalt on resin	
Stirring Speed	
Outputs:	**R^2**
Change in concentration of copper	**0.782**
Change in concentration of cobalt	**0.891**

Comparing ANFIS 5 and 6 to 3 and 4 reveals that the R square values increased when the individual loadings were used instead of one total loading. Using ANFIS 5 and 6 resulted in the most accurate simulations, indicating that a distinction should be made between the loaded species. The increased accuracy of the model is ascribed to the

physical differences in ion exchange between Co and Na, and Co and Cu on the resin surface. By incorporating both Na and Cu loading, the model can distinguish between these mechanisms in the training stage.

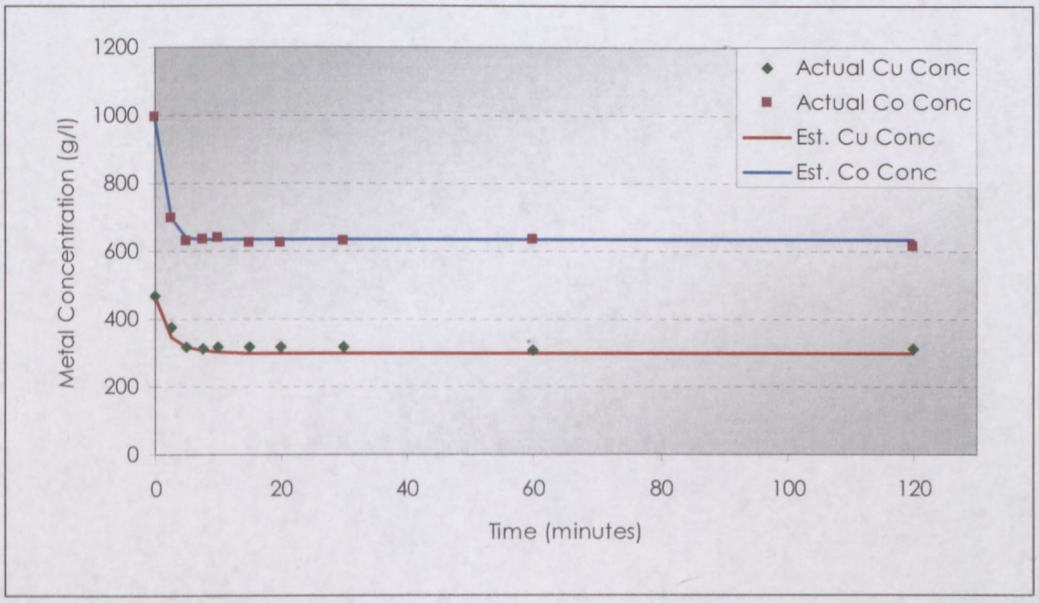

Figure 5.13: ANFIS 5 - The sorption of 500 mg/l copper and 1000 mg/l cobalt onto 10 ml of resin at 120 rpm

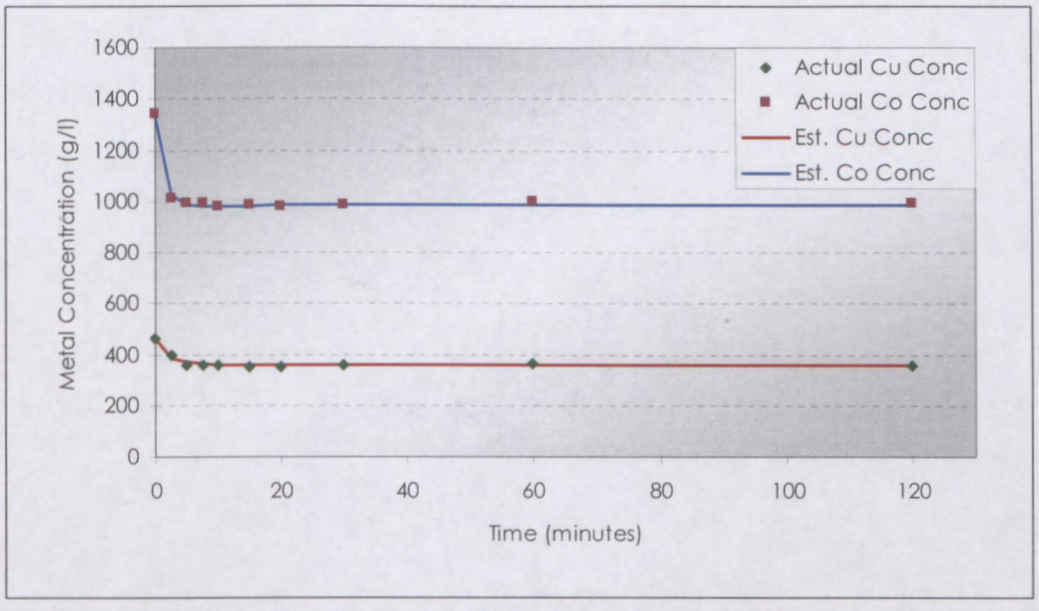

Figure 5.14: ANFIS 5 - The sorption of 500 mg/l copper and 1500 mg/l cobalt onto 10 ml of resin at 200 rpm

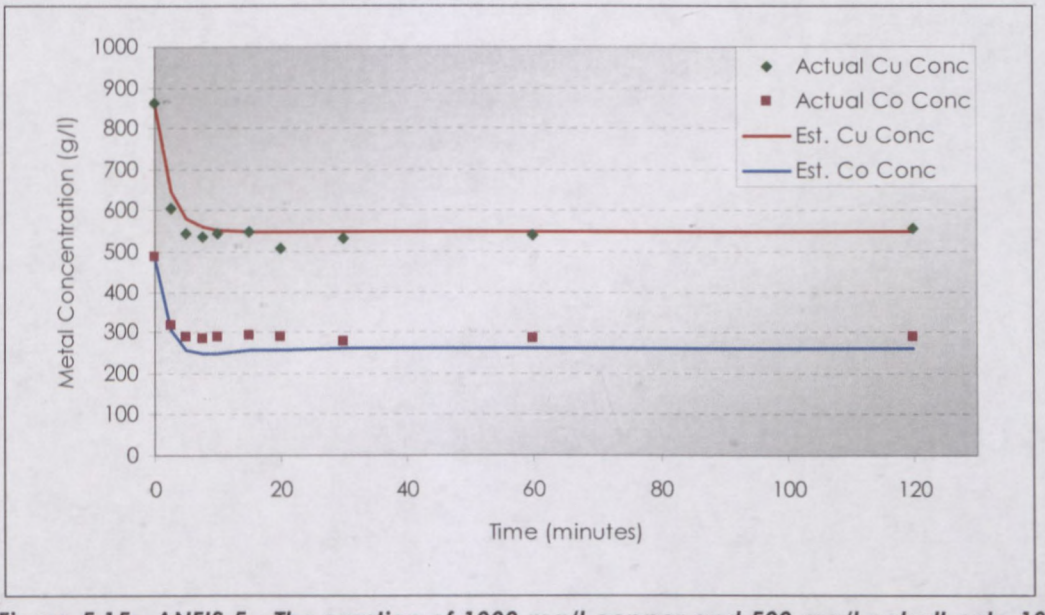

Figure 5.15: ANFIS 5 - The sorption of 1000 mg/l copper and 500 mg/l cobalt onto 10 ml of resin at 300 rpm

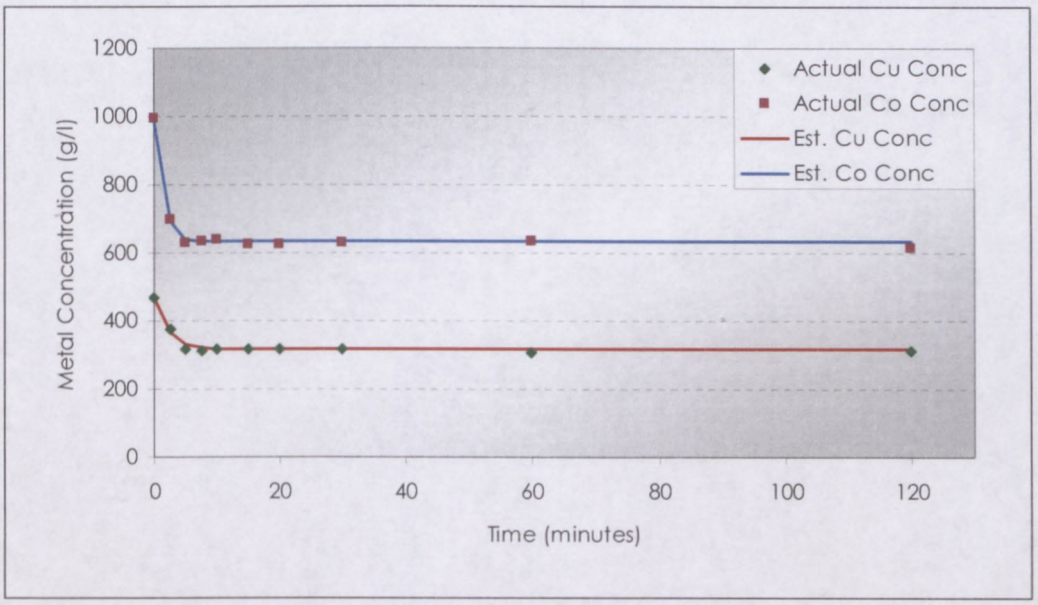

Figure 5.16: ANFIS 6 - The sorption of 500 mg/l copper and 1000 mg/l cobalt onto 10 ml of resin at 120 rpm

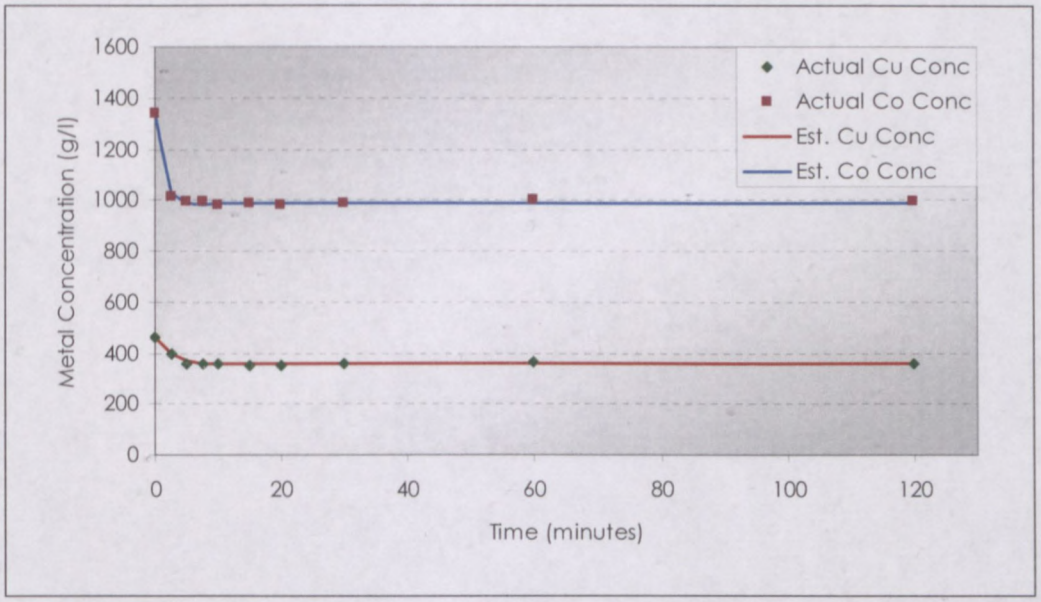

Figure 5.17: ANFIS 6 - The sorption of 500 mg/l copper and 1500 mg/l cobalt onto 10 ml of resin at 200 rpm

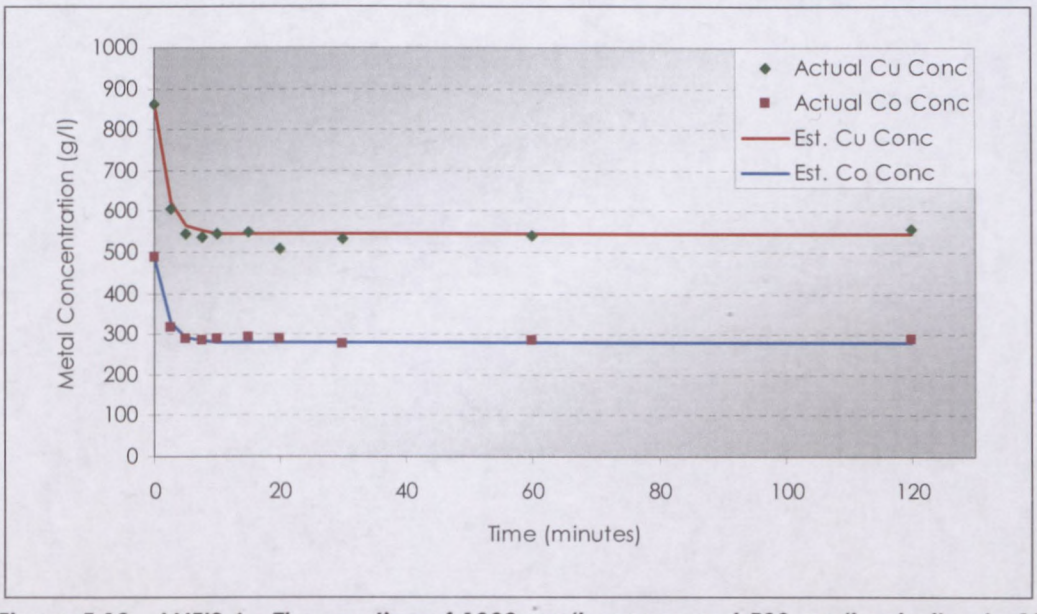

Figure 5.18: ANFIS 6 - The sorption of 1000 mg/l copper and 500 mg/l cobalt onto 10 ml of resin at 300 rpm

5.4 ANFIS 7 & 8: Model with 5 Inputs

Once again, the metal concentrations and the individual metal loadings were used as inputs to the system, excluding stirring speed but including total metal loading on the resin. Hence, in this case a distinction is made between the loading of each species and also the total capacity of the resin utilised.

SOLVER 1

ANFIS 7: Model with 5 Inputs

Inputs:
Concentration of copper
Concentration of cobalt
Loading of copper on resin
Loading of cobalt on resin
Total metal loading on resin

Outputs:	R^2
Change in concentration of copper	**0.747**
Change in concentration of cobalt	**0.869**

SOLVER 2

ANFIS 8: Model with 5 Inputs

Inputs:	
Concentration of copper	
Concentration of cobalt	
Loading of copper on resin	
Loading of cobalt on resin	
Total metal loading on resin	
Outputs:	R^2
Change in concentration of copper	**0.760**
Change in concentration of cobalt	**0.868**

The R^2 values obtained by including the individual loadings did not produce significantly larger R^2 values. In fact, three of the four R^2 values obtained are lower than those for ANFIS 5 and 6. This shows that individual ion exchange mechanisms are more important in the ANFIS training step than total resin capacity.

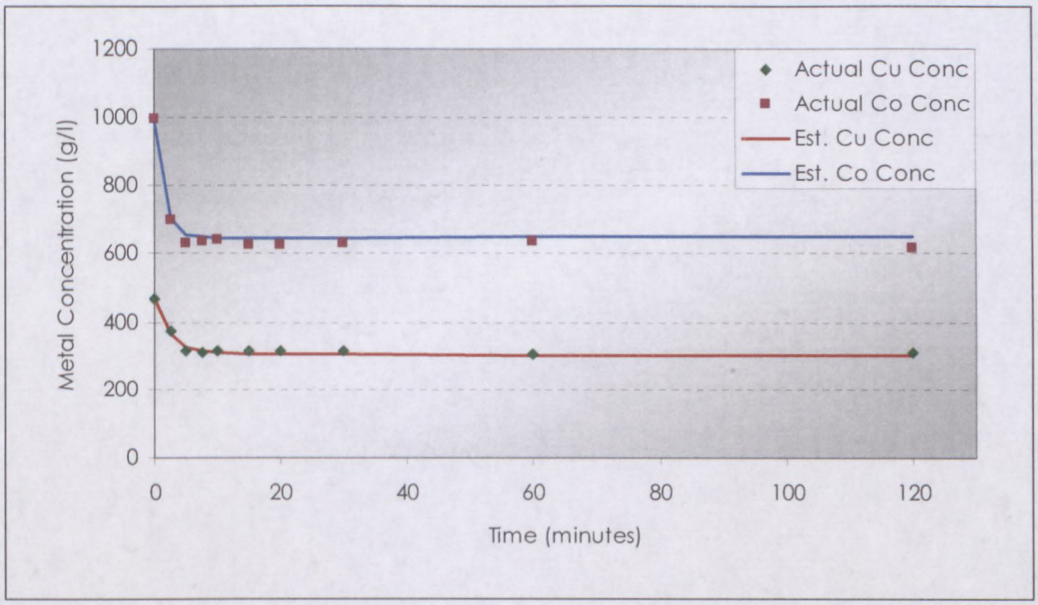

Figure 5.19: ANFIS 7 - The sorption of 500 mg/l copper and 1000 mg/l cobalt onto 10 ml of resin at 120 rpm

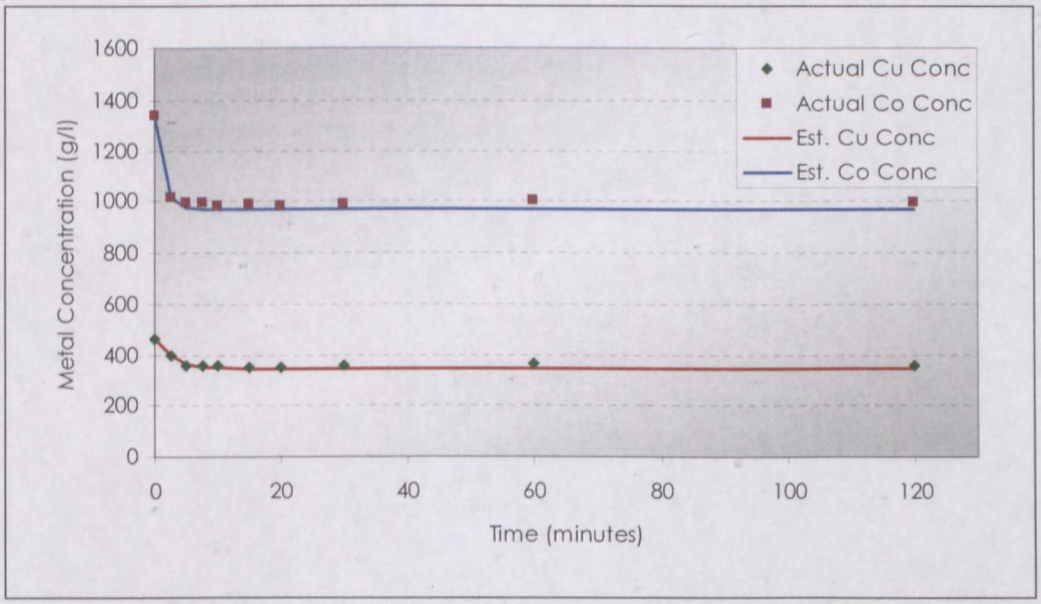

Figure 5.20: ANFIS 7 - The sorption of 500 mg/l copper and 1500 mg/l cobalt onto 10 ml of resin at 200 rpm

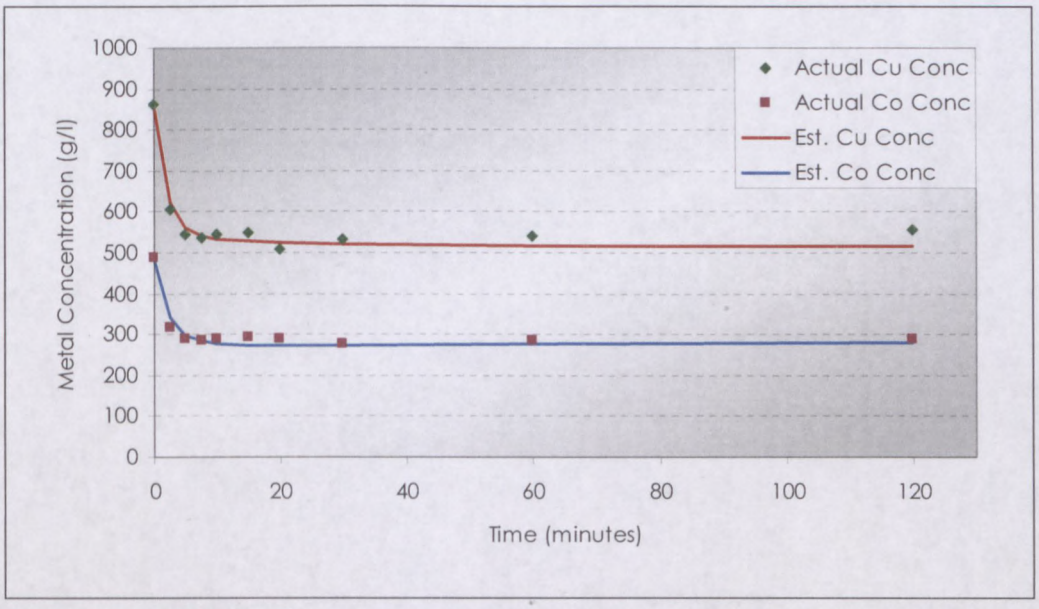

Figure 5.21: ANFIS 7 - The sorption of 1000 mg/l copper and 500 mg/l cobalt onto 10 ml of resin at 300 rpm

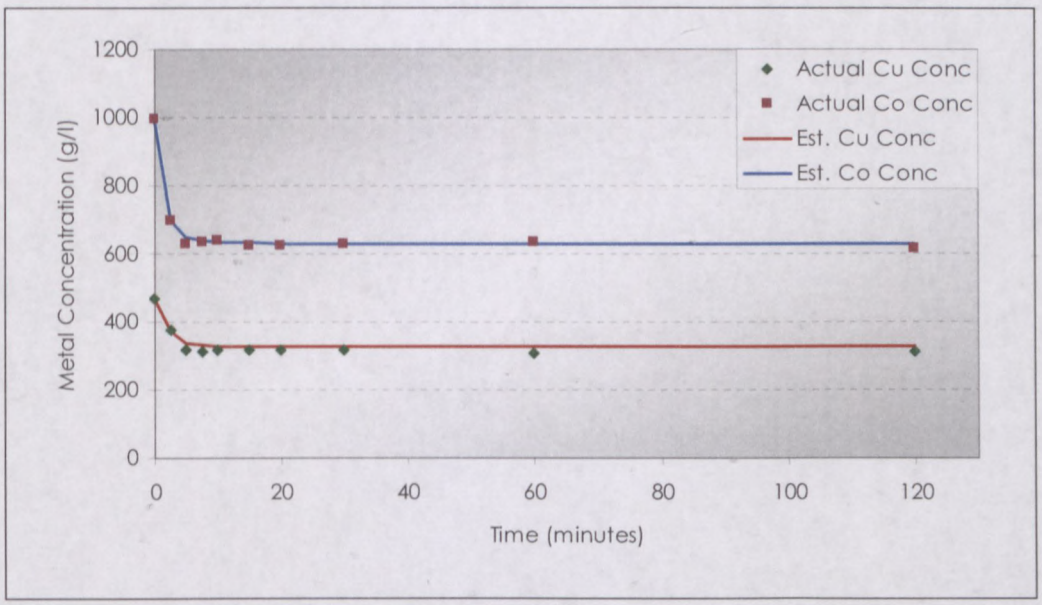

Figure 5.22: ANFIS 8 - The sorption of 500 mg/l copper and 1000 mg/l cobalt onto 10 ml of resin at 120 rpm

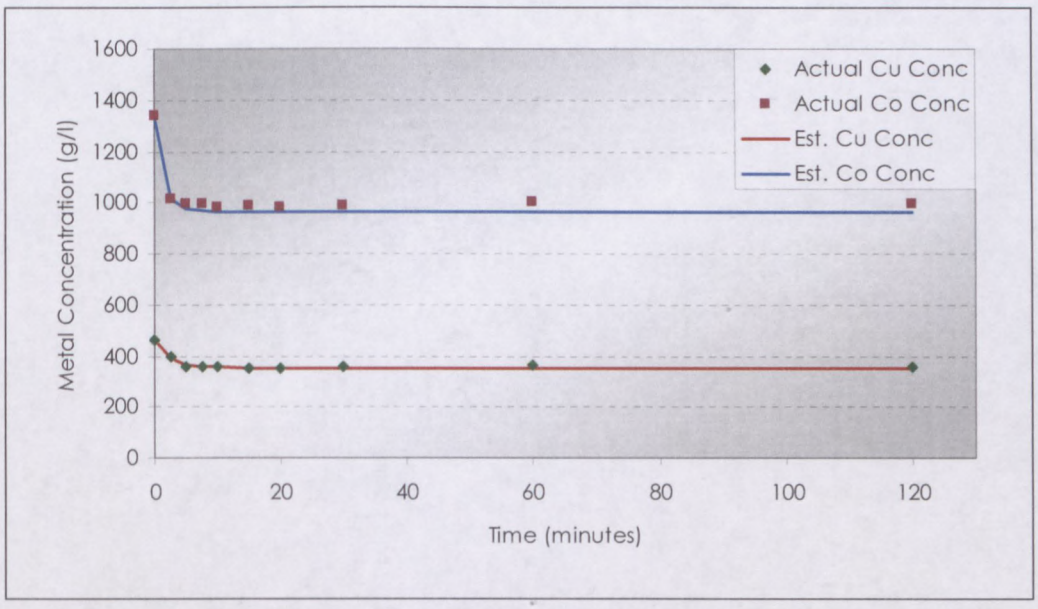

Figure 5.23: ANFIS 8 - The sorption of 500 mg/l copper and 1500 mg/l cobalt onto 10 ml of resin at 200 rpm

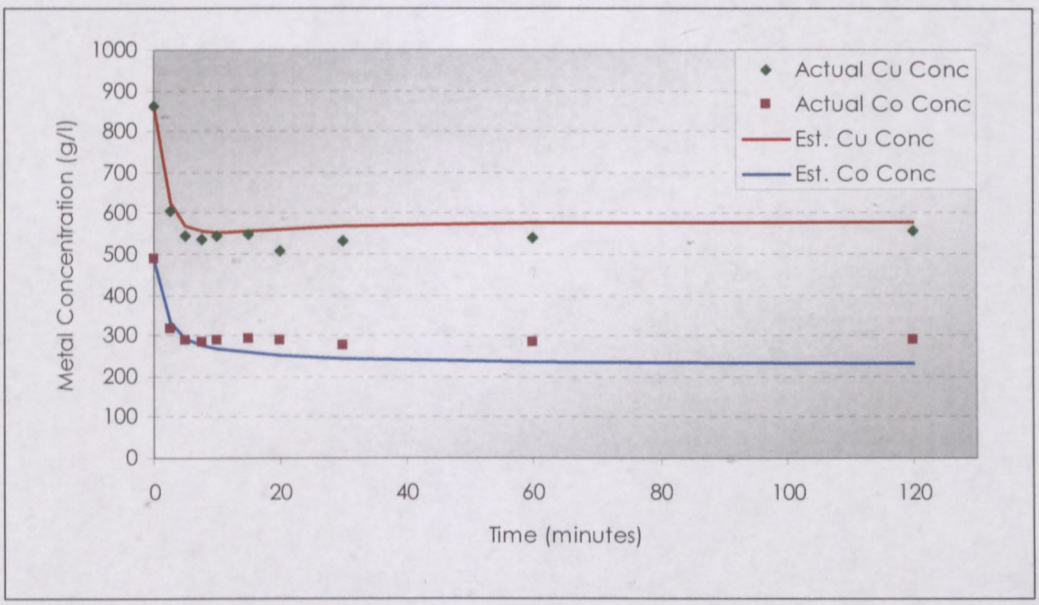

Figure 5.24: ANFIS 8 - The sorption of 1000 mg/l copper and 500 mg/l cobalt onto 10 ml of resin at 300 rpm

5.5 Comparing different ANFIS STRUCTURES STATISTICALLY

The summary of errors obtained from all the ANFIS models are tabulated in Tables 5.2 to 5.9. The simulations of certain experiments gave unrealistic results which are indicated in the grey cells in Tables 5.2 to 5.9. These unrealistic predictions were omitted for the statistical analysis. The unrealistic simulations in certain cases were the first indication that a neuro-fuzzy approach is not an ideal approach for sorption kinetics or that the search algorithm applied was inappropriate. The other reason for the failed attempts could also have been due to over training.

Table 5.2: Percentage error simulating with ANFIS 1

Experiment number	% Error Cobalt	% Error Copper	Average % Error for experiment
1			
2	13.33	4.76	9.04
3			
4	11.44	5.50	8.47
5	2.32	2.51	2.42
6	9.04	7.66	8.35
7	4.99	19.00	12.00
8	4.88	9.51	7.20
9			
10			
11	17.48	8.72	13.10
12	3.49	2.35	2.92
13	2.72	5.80	4.26
14	2.79	6.82	4.80
15	5.78	3.34	4.56
16	5.70	16.64	11.17
17	7.28	13.42	10.35
18			
19			
20	19.45	14.28	16.87
21	7.23	2.59	4.91
22	3.46	2.23	2.85
23	6.46	2.44	4.45
24	10.01	4.67	7.34
25			
26			
27			
Total Average % Error	**7.66**	**7.35**	**7.50**

Table 5.3: Percentage error simulating with ANFIS 2

Experiment number	% Error Cobalt	% Error Copper	Average % Error for experiment
1			
2	1.82	1.60	1.71
3	1.84	1.88	1.86
4	14.37	4.25	9.31
5	5.52	7.47	6.49
6	10.21	6.15	8.18
7	4.95	12.40	8.67
8	3.17	6.28	4.73
9			
10	15.74	21.57	18.66
11	6.33	3.39	4.86
12	5.76	0.79	3.28
13	0.83	2.57	1.70
14	6.74	10.95	8.84
15	3.26	1.07	2.16
16	3.31	10.22	6.77
17	7.47	10.77	9.12
18	2.87	5.92	4.40
19			
20	23.23	14.17	18.70
21	5.99	3.27	4.63
22	2.42	3.75	3.09
23	9.66	5.66	7.66
24	5.75	3.31	4.53
25	4.19	9.77	6.98
26	2.22	4.52	3.37
27	2.06	2.10	2.08
Total Average % Error	**6.24**	**6.41**	**6.32**

Table 5.4: Percentage error simulating with ANFIS 3

Experiment number	% Error Cobalt	% Error Copper	Average % Error for experiment
1			
2	3.56	1.32	2.44
3	4.65	2.88	3.76
4	12.97	43.40	28.18
5	13.34	12.65	13.00
6			
7	9.05	35.44	22.24
8	2.41	4.22	3.32
9			
10	4.33	7.34	5.84
11	14.38	3.55	8.97
12	4.73	2.03	3.38
13	10.78	26.84	18.81
14	7.33	8.89	8.11
15			
16	8.34	27.42	17.88
17	11.81	5.63	8.72
18	11.26	7.07	9.16
19			
20	18.96	10.61	14.79
21			
22	5.19	4.60	4.89
23	7.15	4.00	5.58
24			
25	7.05	19.21	13.13
26			
27			
Total Average % Error	**8.74**	**12.62**	**10.68**

Table 5.5: Percentage error simulating with ANFIS 4

Experiment number	% Error Cobalt	% Error Copper	Average % Error for experiment
1			
2	6.87	1.83	4.35
3	1.52	1.69	1.60
4	9.42	29.69	19.55
5	3.71	3.62	3.67
6			
7	2.35	15.44	8.90
8	2.38	2.80	2.59
9			
10			
11	12.06	4.18	8.12
12	5.38	3.17	4.27
13	7.17	17.34	12.26
14	5.23	7.62	6.42
15	5.32	5.05	5.19
16	1.41	4.20	2.81
17	12.11	5.16	8.63
18	5.01	2.15	3.58
19			
20			
21	5.77	3.33	4.55
22	5.38	3.17	4.27
23			
24			
25			
26	3.71	6.43	5.07
27	3.82	2.46	3.14
Total Average % Error	**5.48**	**6.63**	**6.05**

Table 5.6: Percentage error simulating with ANFIS 5

Experiment number	% Error Cobalt	% Error Copper	Average % Error for experiment
1			
2	4.38	1.15	2.77
3	1.37	1.47	1.42
4	7.61	9.83	8.72
5	2.44	1.96	2.20
6	10.16	6.17	8.16
7	1.48	3.36	2.42
8	2.23	4.01	3.12
9			
10	1.66	9.23	5.44
11	3.22	1.19	2.21
12	1.25	0.66	0.95
13	3.49	4.21	3.85
14	2.60	2.73	2.67
15	2.07	0.84	1.45
16	2.29	6.48	4.38
17	8.59	10.16	9.38
18	3.47	2.99	3.23
19	12.85	108.34	60.59
20	16.39	11.77	14.08
21	4.38	0.99	2.69
22	3.17	8.85	6.01
23	4.10	3.73	3.92
24	5.94	1.67	3.80
25	1.96	5.23	3.59
26	1.51	4.85	3.18
27	2.22	26.54	14.38
Total Average % Error	**4.43**	**9.54**	**6.98**

Table 5.7: Percentage error simulating with ANFIS 6

Experiment number	% Error Cobalt	% Error Copper	Average % Error for experiment
1			
2	1.60	0.98	1.29
3	1.10	1.44	1.27
4	6.17	8.99	7.58
5	1.28	0.75	1.01
6	10.46	6.34	8.40
7	1.55	1.68	1.62
8	2.22	3.20	2.71
9			
10	2.83	14.54	8.69
11	6.14	1.09	3.62
12	1.01	0.66	0.83
13	3.15	2.32	2.73
14	2.01	2.53	2.27
15	1.67	0.78	1.23
16	1.93	5.18	3.56
17	8.30	10.26	9.28
18	2.00	3.73	2.87
19	10.02	13.05	11.53
20	16.59	13.33	14.96
21	5.65	1.01	3.33
22	2.15	2.07	2.11
23	3.72	2.62	3.17
24	5.42	1.61	3.52
25	1.93	3.64	2.79
26	1.00	1.89	1.44
27	2.03	1.84	1.94
Total Average % Error	**4.08**	**4.22**	**4.15**

Table 5.8: Percentage error simulating with ANFIS 7

Experiment number	% Error Cobalt	% Error Copper	Average % Error for experiment
1			
2	2.30	2.38	2.34
3	1.80	1.63	1.72
4	10.45	4.46	7.45
5	1.56	0.83	1.20
6	11.53	5.06	8.30
7			
8	2.40	2.53	2.46
9			
10			
11	3.56	1.52	2.54
12	2.47	1.70	2.08
13	1.81	5.70	3.76
14	2.06	3.47	2.77
15	1.82	1.15	1.48
16			
17	6.65	12.00	9.33
18	2.50	3.80	3.15
19			
20	15.60	17.16	16.38
21	3.56	1.56	2.56
22	2.92	3.47	3.20
23	3.45	3.27	3.36
24	5.12	1.65	3.38
25			
26	1.24	0.63	0.93
27	2.53	1.97	2.25
Total Average % Error	**4.27**	**3.80**	**4.03**

Table 5.9: Percentage error simulating with ANFIS 8

Experiment number	% Error Cobalt	% Error Copper	Average % Error for experiment
1			
2	3.81	0.97	2.39
3	2.01	1.58	1.79
4	14.11	6.33	10.22
5	1.03	1.86	1.44
6	10.73	5.71	8.22
7	1.76	3.83	2.80
8	2.36	2.76	2.56
9			
10			
11	8.06	3.49	5.78
12	1.01	2.13	1.57
13	2.70	11.18	6.94
14	2.04	4.77	3.40
15	1.68	1.14	1.41
16			
17	6.56	11.91	9.24
18	1.98	4.79	3.38
19			
20	18.79	15.51	17.15
21	2.37	1.37	1.87
22	4.09	9.05	6.57
23	5.52	2.58	4.05
24	4.88	1.80	3.34
25			
26	1.38	0.91	1.15
27	2.36	2.39	2.38
Total Average % Error	**4.73**	**4.57**	**4.65**

The average error per experimental set ranges from 4.12 to 10.68 %, which is considered reasonable for a multi-component sorption data prediction. The values for R^2, indicating the correlation values, range from 0.67 up to 0.89.

Overall the correlation values for copper seem to be lower than for cobalt, which, as mentioned before, is probably due to higher selectivity of the resin towards cobalt. The experimental data seems to indicate that the cobalt replaces the copper on the surface of the resin as equilibrium is reached, which increases the complexity of the copper sorption rate, consequently causing the R^2 values for copper to be lower.

When comparing ANFIS 1, 3, 5, 7 and ANFIS 2, 4, 6, 8, it does not seem that the stirring speed has a positive effect on the R^2 values. In fact, when comparing ANFIS 1 and 3, it seems that the inclusion of the stirring speeds increases the average percentage error.

Also, the second training method (i.e. SOLVER 2) gives slightly better results. This hypothesis was statically tested by comparing the mean values of the average percentage errors for SOLVER 1 and for SOLVER 2.

Average % Error (SOLVER 1): $\frac{7.50+10.67+6.98+4.03}{4} = 7.30$

Average % Error (SOLVER 2): $\frac{6.32+6.05+4.15+4.65}{4} = 5.29$

H0: $\mu_{Solver1} = \mu_{Solver2} = 7.30$

H1: $\mu_{Solver2} > \mu_{Solver1}$, hence $\mu_{Solver2} < 7.30$

$\sigma = 0.94$

$\sigma_m = \frac{\sigma}{\sqrt{sample-size}} = \frac{0.92}{\sqrt{4}} = 0.46$

$Z = \frac{5.29-7.30}{0.46} = -4.37 \rightarrow 4.37$

From Appendix C = 0.5

0.5 – 0.5 = 0

0 < 0.01

The Null hypothesis was rejected with 99.9 % confidence. It is concluded that the SOLVER 2 training method provided better results based on the average percentage error.

After concluding that SOLVER 2 should be the training method for modelling, the next step is to test what combination of inputs would statistically provide better results. Here, ANFIS 4 and 6 are compared statically:

H0: $\mu_{ANFIS4} = \mu_{ANFIS6} = 6.05$

H1: $\mu_{ANFIS6} < \mu_{ANFIS4}$, hence $\mu_{ANFIS6} < 6.05$

$\sigma = 3.71$

$$\sigma_m = \frac{\sigma}{\sqrt{sample - size}} = \frac{3.71}{\sqrt{22}} = 0.79$$

$$Z = \frac{4.15 - 6.05}{0.79} = -2.41 \rightarrow 2.41$$

From Appendix C = 0.4918

0.5 – 0.4918 = 0.0082

0.0082 < 0.01

The Null hypothesis was rejected with 99.9% confidence and it is concluded that the mean average error obtained from ANFIS 6 is less than for ANFIS 4. Similar results were obtained when ANFIS 2 and 4, 6 and 8 were compared. It was concluded that the better results were obtained from ANFIS 6 which incorporated five inputs, one of them being stirring speed. This result is consistent with mass transfer theory, where an increase in agitation rate reduces the thickness of the

laminar layer surrounding the particle, increasing the rate of mass transfer.

Moderately good results were obtained from the Adaptive neuro fuzzy inference system programmed in MS EXCEL, although the reason for certain unsuccessful attempts was still unknown. It was concluded that the reason for this was either that the ANFIS concept cannot be applied to this type of process, or the training algorithm used was inappropriate for training. This was confirmed by using a similar system, which is commercially available. The major difference between the two systems is the training method. Instead of using a Newtonian search algorithm, the backpropagation algorithm was used to optimise the ANFIS.

5.6 ANFIS simulations using MATLAB Fuzzy Logic Toolbox

MATLAB is a highly technical language, which can be used to solve complex computing problems and due to its wide range of available applications, is faster than traditional programming languages. One of the available features of MATLAB is the Fuzzy Logic Toolbox, which includes ANFIS functionality.

The ANFIS function in the Fuzzy Logic Toolbox requires a training data set consisting of a chosen number of inputs and one output. Once the training data is loaded, the user can change the default training options such as the type of membership functions, the number of epochs, the training error goal and the step size.

The available options for the MATLAB fuzzy inference system were kept as close as possible to the original system (using MS EXCEL); only the training method was changed to ascertain whether the training

method used in the previous system was inappropriate. To avoid causing over fitting on the training data, especially when using a large number of iterations, a section of the database was introduced as a validation set, which was used to cross-validate the fuzzy inference system. Once training stopped, the fuzzy inference system was saved to use for the generation of ion exchange profiles.

A system similar to ANFIS 6 was created in MATLAB, which generated the results as presented in Figures 5.25 to 5.27.

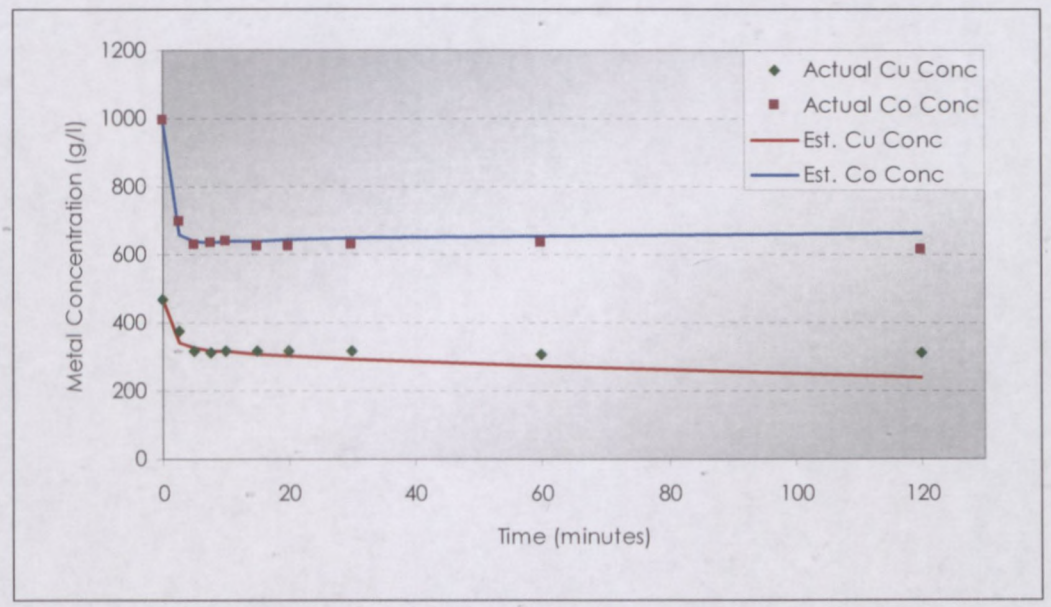

Figure 5.25: MATLAB ANFIS - The sorption of 1000 mg/l copper and 500 mg/l cobalt onto 10 ml of resin at 300 rpm

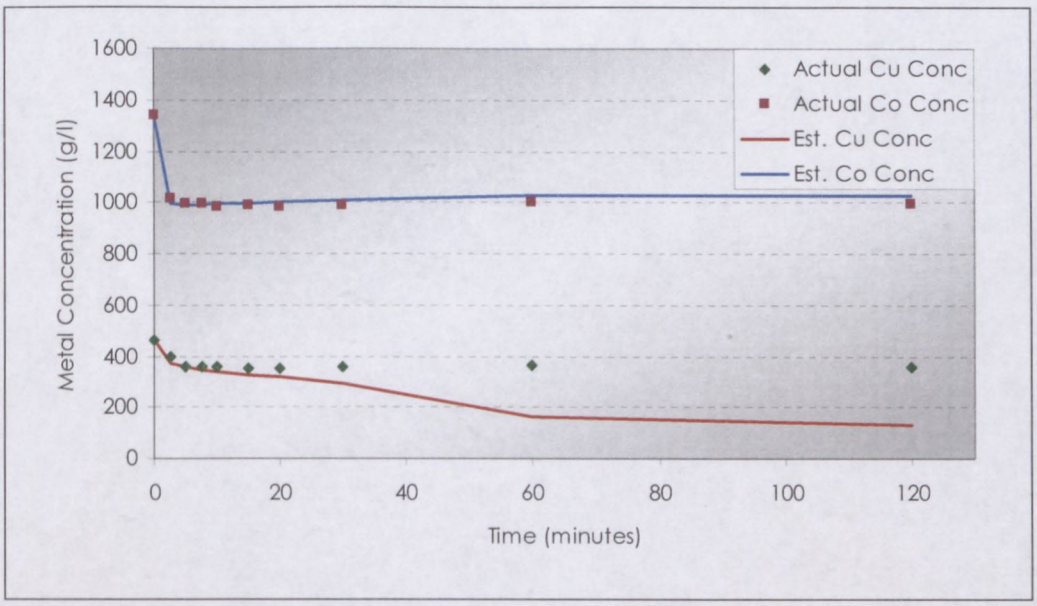

Figure 5.26: MATLAB ANFIS - The sorption of 500 mg/l copper and 1500 mg/l cobalt onto 10 ml of resin at 200 rpm

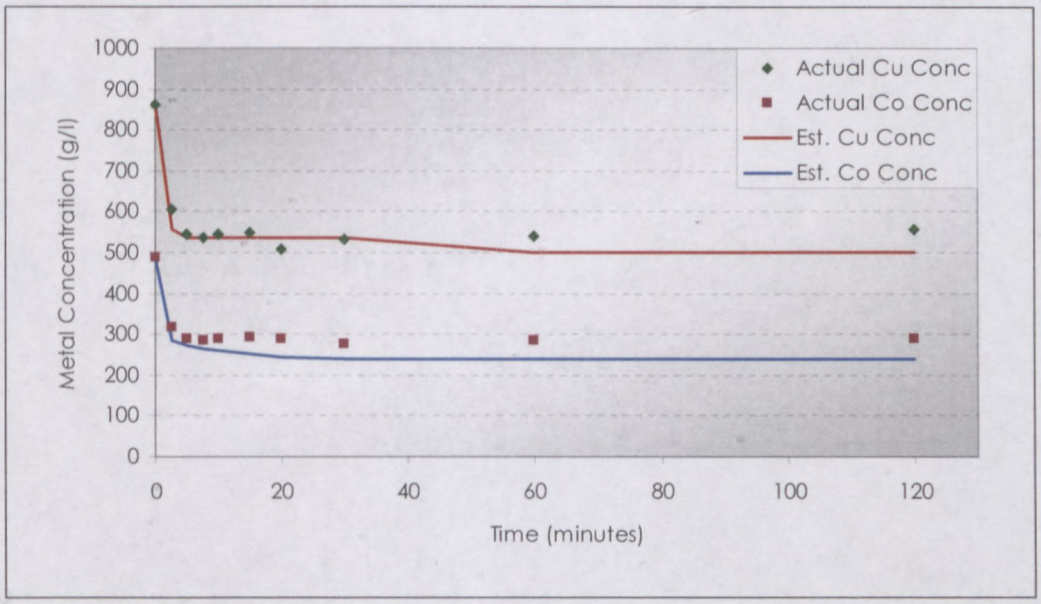

Figure 5.27: MATLAB ANFIS - The sorption of 1000 mg/l copper and 500 mg/l cobalt onto 10 ml of resin at 300 rpm

Table 5.37: Percentage error simulating with MATLAB

Experiment number	% Error Cobalt	% Error Copper	Average % Error for experiment
1			
2	6.29	2.72	4.51
3	13.08	2.04	7.56
4	3.62	4.70	4.16
5	1.86	4.86	3.36
6	2.09	2.28	2.19
7			
8			
9			
10			
11	13.65	4.67	9.16
12	17.08	1.62	9.35
13			
14	4.96	3.47	4.21
15	4.91	2.74	3.83
16			
17	1.97	10.16	6.07
18	8.52	4.53	6.52
19	8.52	4.53	6.52
20			
21			
22	3.84	10.85	7.34
23			
24	12.71	1.76	7.23
25	5.75	13.44	9.60
26	1.50	8.33	4.91
27	2.48	1.88	2.18
Total Average % Error	6.64	4.98	5.81

Again, certain experimental predictions resulted in unrealistic simulated values. As done previously, the results obtained from the simulations were compared statically.

H0: $\mu_{MATLAB} = \mu_{ANFIS6} = 5.81$

H1: $\mu_{ANFIS6} < \mu_{MATLAB}$, hence $\mu_{ANFIS6} < 5.81$

$\sigma = 3.71$

$$\sigma_m = \frac{\sigma}{\sqrt{sample - size}} = \frac{3.71}{\sqrt{21}} = 0.81$$

$$Z = \frac{4.15 - 5.81}{0.81} = -2.05 \rightarrow 2.05$$

From Appendix C = 0.4798

0.5 – 0.4798 = 0.0202

It can be concluded with 99.9% confidence that ANFIS 6 was more accurate than the MATLAB results. This confirms that the search algorithm applied originally was not the major cause for unrealistic results in major cases.

As mentioned earlier, certain simulations gave unrealistic predictions. To test the hypothesis that the training algorithm is to responsible for this phenomenon, a similar procedure was followed using a MATLAB fuzzy logic functionality, which uses a different algorithm. The other possibility for failure could be over-training which was singled out by introducing a test-set in the MATLAB. When the results did not improve it was concluded that the Neuro-Fuzzy approach to sorption processes might not be an ideal prediction tool.

5.7 Comparing FILM DIFFUSION with ANFIS

Both the film diffusion model and ANFIS architecture provided accurate predictions as illustrated in Table 5.38. Statistically, ANFIS 6, the better artificial model, provides a lower percentage error when compared with those obtained from the film diffusion model.

Table 5.38: Percentage errors simulating with the film diffusion model

Experiment number	% Error Cobalt	% Error Copper	Average % Error for experiment
1	2.91	15.22	9.07
2	8.14	3.56	5.85
3	10.47	1.71	6.09
4	2.21	5.05	3.63
5	4.53	1.86	3.20
6	6.62	7.18	6.90
7	4.35	4.46	4.41
8	3.70	3.71	3.71
9	2.85	4.17	3.51
10	7.52	8.60	8.06
11	5.81	1.91	3.86
12	11.96	2.39	7.18
13	12.25	9.15	10.70
14	4.92	3.57	4.25
15	5.51	2.25	3.88
16	9.92	7.37	8.65
17	8.79	10.15	9.47
18	1.70	4.99	3.35
19	14.08	5.66	9.87
20	11.33	16.95	14.14
21	14.12	1.15	7.64
22	10.30	6.16	8.23
23	3.79	3.49	3.64
24	8.73	1.90	5.32
25	6.13	5.12	5.63
26	2.34	2.16	2.25
27	2.32	3.06	2.69
Total Average % Error	**6.94**	**5.29**	**6.12**

H0: $\mu_{diffusion} = \mu_{ANFIS6} = 6.12$

H1: $\mu_{diffusion} > \mu_{ANFIS6}$, hence $\mu_{ANFIS6} < 6.12$

$\sigma = 3.71$

$$\sigma_m = \frac{\sigma}{\sqrt{sample - size}} = \frac{3.71}{\sqrt{26}} = 0.73$$

$$Z = \frac{4.15 - 6.12}{0.73} = -2.7 \rightarrow 2.7$$

From Appendix C = 0.4965

0.5 – 0.4965 = 0.0035

0.0035 < 0.01

The null hypothesis can be rejected with 99.9% confidence, thereby concluding that the artificial model, ANFIS 6, provides more accurate simulations.

Although ANFIS is more accurate, knowledge of programming or a specialised computer package is required. Furthermore, ANFIS does not guarantee a reasonable result, with unrealistic simulations obtained at various stages of the process.

A film diffusion model on the other hand is easier to construct programmatically but does not rely on an accurate equilibrium isotherm.

6 CONCLUSIONS AND RECOMMENDATIONS

The primary aim of this research was to test neuro-fuzzy reasoning as a modelling technique for complex ion exchange processes, the obtained results were then compared with conventional ion exchange modelling techniques. The comparison was based on data sets obtained from laboratory scale ion exchange batch experiments.

Firstly, mass transfer parameters were determined for a film diffusion model, which were then used to simulated ion exchange profiles for copper and cobalt. Before commencing the design of the neuro-fuzzy system, the number of rule, inputs and type of membership functions had to be decided upon. Sensible initial values for the neuro-fuzzy parameters were chosen and manipulated (or trained) using MS EXCEL SOLVER. The programme could model up to five inputs and one output.

The results obtained from the film diffusion method did not result in the same accuracy as the neuro-fuzzy system, indicated by the lower percentage error (4.15% by ANFIS 6) obtained. It was also noted that an increase in the number of inputs in the neuro-fuzzy system did not necessarily generate a better ion exchange model. It was found that the combination of the copper and cobalt solution concentrations, the copper and cobalt resin loading and the stirring speed resulted in the most accurate model.

SOLVER which is based on a Newtonian algorithm is a relatively good tool to use for ion exchange modelling and as shown with the results, there was no need to introduce any sophisticated algorithms.

Although developing neuro-fuzzy software is time consuming, it is a very useful tool and can be applied for many different processes. There are many ways in which this method of modelling could be improved. Different types of membership functions (such as the triangular of bell-shape membership functions) could be tested or even more membership functions could be included. Also, the programme could be improved by simulating more than one output at a time. Other factors which could be tested are different training methods and the accuracy of the database.

REFERENCES

Arsham, H. 1990. What-if Analysis in computer simulation models: A comparative survey with some extensions, *Mathematical and Computer Modelling*. 13(1): 101-106.

Babuška, R. 2003. Neuro-fuzzy methods for modelling and identification, *Studies In Fuzziness And Soft Computing*. is this a journal? If so, use italics for name of journal161–186.

Chen, J.P. and Wang, L. 2004. Characterization of metal adsorption kinetic properties in batch and fixed-bed reactors, *Chemosphere 54*, 397–404.

DeSilva, F.J. 1999. Essentials of ion exchange. Proceedings of 25th Annual WQA Conference.

Ferrari-Trecate, G. and Rovattic, R. 2002. Fuzzy systems with overlapping Gaussian concepts: Approximation properties in Sobolev norms. *Fuzzy Sets and Systems*. 130: 137–145.

Gabrys, B. 2002. Neuro-fuzzy approach to processing inputs with missing values in pattern recognition problems. *International Journal of Approximate Reasoning*. 30: 149-179.

Freundlich, H. 1926. Colloid and capillary chemistry. Methuen.

Fritz, W. and Schluender, E.U. 1974. Simultaneous adsorption equilibria of organic solutes in dilute aqueous solutions on activated carbon, *Chem. Eng. Sc.* 29, 1279-1282.

Helfferich, F.G. 1962. *Ion Exchangers*. New York: McGraw-Hill Book Company, Inc.

Jang, J.S.R., Sun, C.T. and Mizutani, E. 1997. *Neuro-Fuzzy and Soft Computing; a Computational Approach to Learning and Machine Intelligence*. Upper Saddle River: Prentice-Hall,

Jang, J.S.R. 1993. ANFIS: Adaptive network-based fuzzy inference system. *IEEE Transactions on Systems, Man and Cybernetics.* 23: 665-685.

Ling, D., Wu, G., Yang, S. and Zhou Z. 2004. Computer simulation of diffusion of metal ions in resins phenomenological analysis of diffusion process, *Reactive & Functional Polymers.* 61:81–90.

Nauck, D. and Kruse, R. 1999. Neuro-fuzzy systems for function approximation. *Fuzzy Sets and Systems.* 101: 261-271.

Nauck, D. DATE? Beyond Neuro-Fuzzy: Perspectives and Directions, Paper of Third European Congress on Intelligent Techniques and Soft Computing, Aachen.

Nayak, P.C., Sudheerb, K.P., Ranganc, D.M. and Ramasastrid K.S. 2004. A neuro-fuzzy computing technique for modelling hydrological time series. *Journal of Hydrology/* 291: 52–66.

Pedrycz, W. and Waletzky, J. 1997. Fuzzy Clustering with partial supervision. *IEEE Proceedings of the SMC.* Part B, 27(5): 787-795.

Remco. 1981. Ion Exchange, Control and Treatment Technology for the Metal Finishing Industry, 7, 4-10. http://www.remco.com/ix-systs.htm [25 February 2004]

Microsoft Knowledge Base Article – 82890,
www.solver.com [30 February 2004]

Takagi, T. and Sugeno, M. 1985. Fuzzy identification of systems and its applications to modelling and control. *IEEE Transactions Systems Man Cybernetic.*, 15(1): 116--132.

Testing standard deviation, 2004
www.isixsigma.com [13 November 2004]

Van Deventer, J.S.J. 1984. Kinetic model for the adsorption of metal cyanides on activated carbon, Ph.D Thesis: University of Stellenbosch.

Wolfgang, H. Höll. Fundamentals of Ion Exchange Lecture Notes"Forschungszentrum Karlsruhe, Institute for Technical Chemistry, Section WGT, P.O. Box 3640, D-76021, Karlsruhe, Germany.

Zeng, Z., Gu, D., Anthony, R.G. and Klavetter, E. 1995. Estimation of cesium ion exchange distribution coefficients for concentrated electrolytic solutions when using crystalline silicotitamates. *Ind. Eng. Chem. Res.* 34(6): 2142-2147.

APPENDICES

APPENDIX A: TABULATION OF EXPERIMENTAL & SIMULATED DATA

Table A.1: Film Diffusion Simulations for Experiment 2

Time	Actual Cu Conc	Actual Co Conc	Est. Cu Conc	Est. Co Conc
(min)			*(mg/l)*	
0	467.85	993.00	467.85	993.00
2.5	374.80	699.20	357.82	748.74
5	315.25	631.15	297.05	638.30
7.5	313.85	633.10	288.04	647.32
10	319.00	640.00	284.19	651.52
15	316.45	626.40	281.76	654.14
20	316.45	626.40	281.29	654.63
30	317.60	628.65	281.18	654.74
60	308.30	632.05	281.18	654.75
120	310.95	613.95	281.18	654.75

Table A.2: Film Diffusion Simulations for Experiment 12

Time	Actual Cu Conc	Actual Co Conc	Estimated Cu Conc	Estimated Co Conc
(min)			*(mg/l)*	
0	462.10	1341.70	462.10	1341.70
2.5	395.60	1017.80	358.77	1042.65
5	358.20	995.90	316.99	956.00
7.5	357.80	996.30	309.22	958.90
10	360.20	979.00	307.27	963.99
15	352.20	986.20	305.47	964.49
20	351.80	980.80	305.82	966.32
30	354.80	989.20	305.55	965.95
60	364.70	1000.10	305.79	966.54
120	355.90	994.10	305.76	966.49

Table A.3: Film Diffusion Simulations for Experiment 22

Time	Actual Cu Conc	Actual Co Conc	Estimated Cu Conc	Estimated Co Conc
(min)			*(mg/l)*	
0	861.40	485.90	861.40	485.90
2.5	606.20	317.55	658.77	366.10
5	545.25	287.60	507.11	278.60
7.5	537.55	285.35	478.12	267.34
10	544.40	289.05	473.32	267.90
15	549.55	291.45	470.81	268.93
20	510.05	287.00	470.09	269.15
30	533.30	276.90	469.85	269.22
60	542.60	285.10	469.84	269.23
120	557.45	290.50	469.84	269.23

Table A.4: ANFIS 1 Simulation for Experiment 2

Time	Actual Cu Conc	Actual Co Conc	NF Cu Conc	NF Co Conc
(min)	*(mg/l)*			
0	467.85	993.00	467.85	993.00
2.5	374.80	699.20	381.20	705.15
5	315.25	631.15	356.76	641.67
7.5	313.85	633.10	350.15	621.19
10	319.00	640.00	348.66	612.35
15	316.45	626.40	350.16	604.64
20	316.45	626.40	353.23	600.25
30	317.60	628.65	360.12	592.68
60	308.30	632.05	381.94	569.35
120	310.95	613.95	429.01	518.45

Table A.5: ANFIS 1 Simulation for Experiment 12

Time	Actual Cu Conc	Actual Co Conc	NF Cu Conc	NF Co Conc
(min)	*(mg/l)*			
0	462.10	1341.70	462.10	1341.70
2.5	395.60	1017.80	396.06	1030.00
5	358.20	995.90	380.64	975.21
7.5	357.80	996.30	375.73	959.87
10	360.20	979.00	373.62	954.89
15	352.20	986.20	371.62	953.24
20	351.80	980.80	370.25	954.05
30	354.80	989.20	367.69	956.51
60	364.70	1000.10	359.70	964.43
120	355.90	994.10	341.46	982.25

Table A.6: ANFIS 1 Simulation for Experiment 22

Time	Actual Cu Conc	Actual Co Conc	NF Cu Conc	NF Co Conc
(min)	*(mg/l)*			
0	861.40	485.90	861.40	485.90
2.5	606.20	317.55	644.36	329.82
5	545.25	287.60	583.65	290.49
7.5	537.55	285.35	562.80	279.61
10	544.40	289.05	553.79	275.98
15	549.55	291.45	546.81	274.81
20	510.05	287.00	544.10	275.74
30	533.30	276.90	541.10	278.27
60	542.60	285.10	535.45	283.96
120	557.45	290.50	530.15	289.34

Table A.7: ANFIS 2 Simulation for Experiment 2

Time	Actual Cu Conc	Actual Co Conc	NF Cu Conc	NF Co Conc
(min)	*(mg/l)*			
0	467.85	993.00	467.85	993.00
2.5	374.80	699.20	357.93	711.58
5	315.25	631.15	328.70	660.27
7.5	313.85	633.10	322.62	644.70
10	319.00	640.00	320.60	638.43
15	316.45	626.40	319.35	634.40
20	316.45	626.40	318.99	633.60
30	317.60	628.65	318.64	633.62
60	308.30	632.05	317.61	634.65
120	310.95	613.95	314.21	638.11

Table A.8: ANFIS 2 Simulation for Experiment 12

Time	Actual Cu Conc	Actual Co Conc	NF Cu Conc	NF Co Conc
(min)	*(mg/l)*			
0	462.10	1341.70	462.10	1341.70
2.5	395.60	1017.80	375.36	1035.32
5	358.20	995.90	351.64	994.04
7.5	357.80	996.30	345.91	984.57
10	360.20	979.00	343.50	982.31
15	352.20	986.20	340.79	982.90
20	351.80	980.80	338.58	984.81
30	354.80	989.20	334.25	988.99
60	364.70	1000.10	320.93	1001.83
120	355.90	994.10	292.05	1029.08

Table A.9: ANFIS 2 Simulation for Experiment 22

Time	Actual Cu Conc	Actual Co Conc	NF Cu Conc	NF Co Conc
(min)	*(mg/l)*			
0	861.40	485.90	861.40	485.90
2.5	606.20	317.55	617.53	334.30
5	545.25	287.60	562.42	302.41
7.5	537.55	285.35	550.13	292.18
10	544.40	289.05	546.37	287.23
15	549.55	291.45	545.53	282.24
20	510.05	287.00	547.06	279.34
30	533.30	276.90	551.00	275.09
60	542.60	285.10	560.11	266.35
120	557.45	290.50	568.33	258.54

Table A.10: ANFIS 3 Simulation for Experiment 2

Time	Actual Cu Conc	Actual Co Conc	NF Cu Conc	NF Co Conc
(min)	*(mg/l)*			
0	467.85	993.00	467.85	993.00
2.5	374.80	699.20	357.93	711.58
5	315.25	631.15	328.70	660.27
7.5	313.85	633.10	322.62	644.70
10	319.00	640.00	320.60	638.43
15	316.45	626.40	319.35	634.40
20	316.45	626.40	318.99	633.60
30	317.60	628.65	318.64	633.62
60	308.30	632.05	317.61	634.65
120	310.95	613.95	314.21	638.11

Table A.11: ANFIS 3 Simulation for Experiment 12

Time	Actual Cu Conc	Actual Co Conc	NF Cu Conc	NF Co Conc
(min)	*(mg/l)*			
0	462.10	1341.70	462.10	1341.70
2.5	395.60	1017.80	375.36	1035.32
5	358.20	995.90	351.64	994.04
7.5	357.80	996.30	345.91	984.57
10	360.20	979.00	343.50	982.31
15	352.20	986.20	340.79	982.90
20	351.80	980.80	338.58	984.81
30	354.80	989.20	334.25	988.99
60	364.70	1000.10	320.93	1001.83
120	355.90	994.10	292.05	1029.08

Table A.12: ANFIS 3 Simulation for Experiment 22

Time	Actual Cu Conc	Actual Co Conc	NF Cu Conc	NF Co Conc
(min)	*(mg/l)*			
0	861.40	485.90	861.40	485.90
2.5	606.20	317.55	617.53	334.30
5	545.25	287.60	562.42	302.41
7.5	537.55	285.35	550.13	292.18
10	544.40	289.05	546.37	287.23
15	549.55	291.45	545.53	282.24
20	510.05	287.00	547.06	279.34
30	533.30	276.90	551.00	275.09
60	542.60	285.10	560.11	266.35
120	557.45	290.50	568.33	258.54

Table A.13: ANFIS 4 Simulation for Experiment 2

Time	Actual Cu Conc	Actual Co Conc	NF Cu Conc	NF Co Conc
(min)			*(mg/l)*	
0	467.85	993.00	467.85	993.00
2.5	374.80	699.20	364.67	709.32
5	315.25	631.15	332.54	654.83
7.5	313.85	633.10	326.97	641.62
10	319.00	640.00	327.29	636.16
15	316.45	626.40	331.24	630.12
20	316.45	626.40	335.50	625.55
30	317.60	628.65	342.89	617.88
60	308.30	632.05	357.72	602.48
120	310.95	613.95	370.26	589.41

Table A.14: ANFIS 4 Simulation for Experiment 12

Time	Actual Cu Conc	Actual Co Conc	NF Cu Conc	NF Co Conc
(min)			*(mg/l)*	
0	462.10	1341.70	462.10	1341.70
2.5	395.60	1017.80	380.01	1033.84
5	358.20	995.90	360.25	986.28
7.5	357.80	996.30	358.18	975.58
10	360.20	979.00	359.60	971.24
15	352.20	986.20	364.11	965.74
20	351.80	980.80	368.75	960.88
30	354.80	989.20	377.64	951.62
60	364.70	1000.10	401.69	926.53
120	355.90	994.10	442.00	884.18

Table A.15: ANFIS 4 Simulation for Experiment 22

Time	Actual Cu Conc	Actual Co Conc	NF Cu Conc	NF Co Conc
(min)			*(mg/l)*	
0	861.40	485.90	861.40	485.90
2.5	606.20	317.55	635.46	311.75
5	545.25	287.60	570.97	275.65
7.5	537.55	285.35	553.48	264.87
10	544.40	289.05	547.27	257.97
15	549.55	291.45	544.80	257.97
20	510.05	287.00	546.50	257.97
30	533.30	276.90	546.50	257.97
60	542.60	285.10	546.50	257.97
120	557.45	290.50	546.50	257.97

Table A.16: ANFIS 5 Simulation for Experiment 2

Time	Actual Cu Conc	Actual Co Conc	NF Cu Conc	NF Co Conc
(min)			*(mg/l)*	
0	467.85	993.00	467.85	993.00
2.5	374.80	699.20	347.12	698.37
5	315.25	631.15	316.82	641.44
7.5	313.85	633.10	305.84	634.05
10	319.00	640.00	300.78	634.12
15	316.45	626.40	297.27	635.70
20	316.45	626.40	296.49	636.29
30	317.60	628.65	296.29	636.48
60	308.30	632.05	296.28	636.49
120	310.95	613.95	296.28	636.49

Table A.17: ANFIS 5 Simulation for Experiment 12

Time	Actual Cu Conc	Actual Co Conc	NF Cu Conc	NF Co Conc
(min)			*(mg/l)*	
0	462.10	1341.70	462.10	1341.70
2.5	395.60	1017.80	382.76	1025.26
5	358.20	995.90	367.71	987.21
7.5	357.80	996.30	361.34	984.41
10	360.20	979.00	358.27	984.75
15	352.20	986.20	356.06	985.32
20	351.80	980.80	355.54	985.47
30	354.80	989.20	355.39	985.51
60	364.70	1000.10	355.38	985.52
120	355.90	994.10	355.38	985.52

Table A.18: ANFIS 5 Simulation for Experiment 22

Time	Actual Cu Conc	Actual Co Conc	NF Cu Conc	NF Co Conc
(min)			*(mg/l)*	
0	861.40	485.90	861.40	485.90
2.5	606.20	317.55	645.00	305.95
5	545.25	287.60	581.00	257.80
7.5	537.55	285.35	560.52	249.32
10	544.40	289.05	552.98	249.75
15	549.55	291.45	548.77	254.46
20	510.05	287.00	547.85	257.58
30	533.30	276.90	547.39	259.71
60	542.60	285.10	547.29	260.21
120	557.45	290.50	547.29	260.21

Table A.19: ANFIS 6 Simulation for Experiment 2

Time	Actual Cu Conc	Actual Co Conc	NF Cu Conc	NF Co Conc
(min)	*(mg/l)*			
0	467.85	993.00	467.85	993.00
2.5	374.80	699.20	365.88	695.00
5	315.25	631.15	333.74	639.75
7.5	313.85	633.10	323.17	633.20
10	319.00	640.00	319.04	633.04
15	316.45	626.40	316.59	633.65
20	316.45	626.40	316.14	633.82
30	317.60	628.65	316.04	633.86
60	308.30	632.05	316.04	633.86
120	310.95	613.95	316.04	633.86

Table A.20: ANFIS 6 Simulation for Experiment 12

Time	Actual Cu Conc	Actual Co Conc	NF Cu Conc	NF Co Conc
(min)	*(mg/l)*			
0	462.10	1341.70	462.10	1341.70
2.5	395.60	1017.80	396.62	1026.57
5	358.20	995.90	370.16	987.43
7.5	357.80	996.30	360.71	985.04
10	360.20	979.00	357.27	985.50
15	352.20	986.20	355.54	985.97
20	351.80	980.80	355.31	986.04
30	354.80	989.20	355.27	986.05
60	364.70	1000.10	355.27	986.05
120	355.90	994.10	355.27	986.05

Table A.21: ANFIS 6 Simulation for Experiment 22

Time	Actual Cu Conc	Actual Co Conc	NF Cu Conc	NF Co Conc
(min)	*(mg/l)*			
0	861.40	485.90	861.40	485.90
2.5	606.20	317.55	623.26	330.93
5	545.25	287.60	565.30	293.05
7.5	537.55	285.35	550.83	284.13
10	544.40	289.05	546.26	281.81
15	549.55	291.45	544.08	281.14
20	510.05	287.00	543.77	281.16
30	533.30	276.90	543.70	281.20
60	542.60	285.10	543.70	281.20
120	557.45	290.50	543.70	281.20

Table A.22: ANFIS 7 Simulation for Experiment 2

Time	Actual Cu Conc	Actual Co Conc	NF Cu Conc	NF Co Conc
(min)			*(mg/l)*	
0	467.85	993.00	467.85	993.00
2.5	374.80	699.20	364.30	702.58
5	315.25	631.15	326.63	656.06
7.5	313.85	633.10	314.71	647.47
10	319.00	640.00	310.11	645.16
15	316.45	626.40	306.94	644.64
20	316.45	626.40	305.89	645.12
30	317.60	628.65	305.09	645.91
60	308.30	632.05	304.59	646.51
120	310.95	613.95	304.55	646.56

Table A.23: ANFIS 7 Simulation for Experiment 12

Time	Actual Cu Conc	Actual Co Conc	NF Cu Conc	NF Co Conc
(min)			*(mg/l)*	
0	462.10	1341.70	462.10	1341.70
2.5	395.60	1017.80	393.53	1012.66
5	358.20	995.90	364.96	973.28
7.5	357.80	996.30	354.33	967.09
10	360.20	979.00	349.31	966.35
15	352.20	986.20	344.84	967.91
20	351.80	980.80	343.12	969.50
30	354.80	989.20	342.15	970.93
60	364.70	1000.10	341.97	971.31
120	355.90	994.10	341.97	971.31

Table A.24: ANFIS 7 Simulation for Experiment 22

Time	Actual Cu Conc	Actual Co Conc	NF Cu Conc	NF Co Conc
(min)			*(mg/l)*	
0	861.40	485.90	861.40	485.90
2.5	606.20	317.55	622.76	340.66
5	545.25	287.60	560.27	297.80
7.5	537.55	285.35	542.26	283.17
10	544.40	289.05	534.43	276.80
15	549.55	291.45	527.47	272.44
20	510.05	287.00	524.27	271.98
30	533.30	276.90	521.02	273.77
60	542.60	285.10	517.55	278.35
120	557.45	290.50	516.63	279.94

Table A.25: ANFIS 8 Simulation for Experiment 2

Time	Actual Cu Conc	Actual Co Conc	NF Cu Conc	NF Co Conc
(min)			*(mg/l)*	
0	467.85	993.00	467.85	993.00
2.5	374.80	699.20	369.70	697.04
5	315.25	631.15	338.25	649.47
7.5	313.85	633.10	330.05	638.93
10	319.00	640.00	327.61	634.95
15	316.45	626.40	326.90	631.97
20	316.45	626.40	327.18	630.87
30	317.60	628.65	327.59	630.09
60	308.30	632.05	327.78	629.78
120	310.95	613.95	327.79	629.77

Table A.26: ANFIS 8 Simulation for Experiment 12

Time	Actual Cu Conc	Actual Co Conc	NF Cu Conc	NF Co Conc
(min)			*(mg/l)*	
0	462.10	1341.70	462.10	1341.70
2.5	395.60	1017.80	390.72	1012.28
5	358.20	995.90	365.76	973.89
7.5	357.80	996.30	358.26	966.06
10	360.20	979.00	355.37	963.61
15	352.20	986.20	353.56	962.49
20	351.80	980.80	353.15	962.44
30	354.80	989.20	353.01	962.54
60	364.70	1000.10	353.00	962.57
120	355.90	994.10	353.00	962.57

Table A.27: ANFIS 8 Simulation for Experiment 22

Time	Actual Cu Conc	Actual Co Conc	NF Cu Conc	NF Co Conc
(min)			*(mg/l)*	
0	861.40	485.90	861.40	485.90
2.5	606.20	317.55	627.97	333.53
5	545.25	287.60	567.78	291.19
7.5	537.55	285.35	556.03	276.06
10	544.40	289.05	554.20	267.96
15	549.55	291.45	557.18	258.41
20	510.05	287.00	561.41	252.14
30	533.30	276.90	568.06	243.81
60	542.60	285.10	576.29	234.00
120	557.45	290.50	578.47	231.45

Table A.28: MATLAB ANFIS Simulation for Experiment 2

Time	Actual Cu Conc	Actual Co Conc	NF Cu Conc	NF Co Conc
(min)			*(mg/l)*	
0	467.85	993.00	467.85	993.00
2.5	374.80	699.20	343.11	658.00
5	315.25	631.15	326.94	637.24
7.5	313.85	633.10	318.79	635.75
10	319.00	640.00	315.40	637.11
15	316.45	626.40	308.78	640.55
20	316.45	626.40	303.46	643.24
30	317.60	628.65	294.89	647.17
60	308.30	632.05	275.17	654.49
120	310.95	613.95	237.41	663.29

Table A.29: MATLAB ANFIS Simulation for Experiment 12

Time	Actual Cu Conc	Actual Co Conc	NF Cu Conc	NF Co Conc
(min)			*(mg/l)*	
0	462.10	1341.70	462.10	1341.70
2.5	395.60	1017.80	369.10	998.15
5	358.20	995.90	355.74	988.41
7.5	357.80	996.30	344.65	991.00
10	360.20	979.00	338.73	993.01
15	352.20	986.20	326.38	997.50
20	351.80	980.80	315.47	1001.60
30	354.80	989.20	291.46	1009.90
60	364.70	1000.10	163.78	1025.90
120	355.90	994.10	131.06	1030.20

Table A.30: MATLAB ANFIS Simulation for Experiment 22

Time	Actual Cu Conc	Actual Co Conc	NF Cu Conc	NF Co Conc
(min)			*(mg/l)*	
0	861.40	485.90	861.40	485.90
2.5	606.20	317.55	555.24	284.50
5	545.25	287.60	535.85	271.10
7.5	537.55	285.35	535.29	265.18
10	544.40	289.05	535.40	261.53
15	549.55	291.45	535.56	252.44
20	510.05	287.00	535.56	243.17
30	533.30	276.90	534.99	240.00
60	542.60	285.10	500.74	239.10
120	557.45	290.50	498.10	239.32

APPENDIX B: AMBERJET 1200 H DATA SHEET

AMBERJET® 1200 H

Industrial Grade Strong Acid Cation Exchanger

Remove banner

PRODUCT DATA SHEET

AMBERJET 1200 H is a uniform particle size, high quality, strong acid cation exchanger designed for use in all general demineralisation systems.
The uniformity and mean particle size of AMBERJET 1200 H have been optimised for use in industrial demineralisation equipment including mixed beds when paired with AMBERJET 4200 Cl. AMBERJET 1200 H can be directly substituted for conventional gel cation exchange resin in new equipment and in rebeds of existing installations.

PROPERTIES

Matrix	Styrene divinylbenzene copolymer
Functional groups	$-SO_3^-$
Physical form	Insoluble, amber beads
Ionic form as shipped	H^+
Total exchange capacity [1]	≥ 1.8 eq/L (H^+ form) - ≥ 2.0 eq/L (Na^+ form)
Moisture holding capacity [1]	49 to 55 % (H^+ form)
Shipping weight	800 g/L
Specific gravity	1.18 to 1.22 (H^+ form)
Uniformity coefficient [1]	≤ 1.2
Harmonic mean size	630 ± 50 µm
Fines content [1]	< 0.300 mm : 0.1 % max
Coarse beads	> 0.850 mm : 10 % max
Maximum reversible swelling	$Na^+ \rightarrow H^+$: 10 %

[1] *Contractual value*
Test methods are available on request.

SUGGESTED OPERATING CONDITIONS

Minimum bed depth	800 mm	
Service flow rate	5 to 50 BV*/h	
Maximum service velocity	60 m/h	
Regenerant	HCl	H_2SO_4
Level	40 to 150	40 to 200
Concentration	4 to 10	1 to 8
Flow rate	2 to 5	2 to 20
Minimum contact time	20 minutes	
Slow rinse	2 BV at regeneration flow rate	
Fast rinse	1 to 3 BV at service flow rate	

** 1 BV (Bed Volume) = 1 m^3 solution per m^3 resin*

RDS 0348 A - Lins 97 - 1/2

PERFORMANCE

Operating capacity and sodium leakage depend on several factors such as water analysis, temperature and regenerant level. The engineering data sheets EDS 0355 A, 0356 A, 0359 A, and 0360 A, provide information to calculate them.

LIMITS OF USE

AMBERJET 1200 H is suitable for industrial uses. For all other specific applications such as pharmaceutical, food processing or potable water applications, it is recommended that all potential users seek advice from Rohm and Haas in order to determine the best resin choice and optimum operating conditions.

HYDRAULIC CHARACTERISTICS

Figure 1 shows the bed expansion of AMBERJET 1200 H as a function of backwash flow rate and water temperature. Figure 2 shows the pressure drop data for AMBERJET 1200 H, as a function of service flow rate and water temperature. Pressure drop data are valid at the start of the service run with a clear water and a correctly classified bed.

Fig. 1 : Bed Expansion

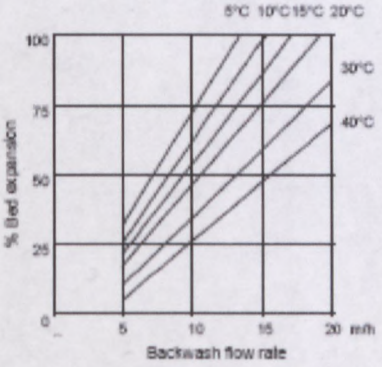

Fig. 2 : Pressure Drop

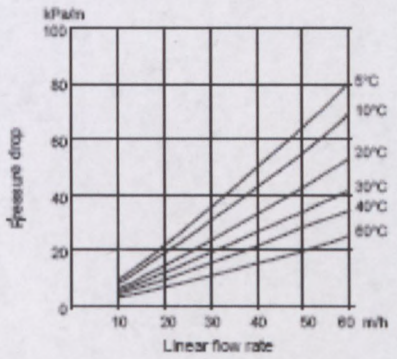

All our products are produced in ISO 9002 certified manufacturing facilities.

Rohm and Haas/Ion Exchange Resins - Philadelphia, PA - Tel. (800) RH AMBER - Fax: (215) 537-4157
Rohm and Haas/Ion Exchange Resins - 75579 Paris Cedex 12 - Tel. (33) 1 40 02 50 00 - Fax: 1 43 45 28 19
WEB SITE: http://www.rohmhaas.com/ionexchange

FDS 0348 A - Line 97 - 2/2

APPENDIX C: TABLE OF STANDARD NORMAL (Z) DISTRIBUTION

z	0.00	0.01	0.02	0.03	0.04	0.05	0.06	0.07	0.08	0.09
0.0	0.0000	0.0040	0.0080	0.0120	0.0160	0.0190	0.0239	0.0279	0.0319	0.0359
0.1	0.0398	0.0438	0.0478	0.0517	0.0557	0.0596	0.0636	0.0675	0.0714	0.0753
0.2	0.0793	0.0832	0.0871	0.0910	0.0948	0.0987	0.1026	0.1064	0.1103	0.1141
0.3	0.1179	0.1217	0.1255	0.1293	0.1331	0.1368	0.1406	0.1443	0.1480	0.1517
0.4	0.1554	0.1591	0.1628	0.1664	0.1700	0.1736	0.1772	0.1808	0.1844	0.1879
0.5	0.1915	0.1950	0.1985	0.2019	0.2054	0.2088	0.2123	0.2157	0.2190	0.2224
0.6	0.2257	0.2291	0.2324	0.2357	0.2389	0.2422	0.2454	0.2486	0.2517	0.2549
0.7	0.2580	0.2611	0.2642	0.2673	0.2704	0.2734	0.2764	0.2794	0.2823	0.2852
0.8	0.2881	0.2910	0.2939	0.2969	0.2995	0.3023	0.3051	0.3078	0.3106	0.3133
0.9	0.3159	0.3186	0.3212	0.3238	0.3264	0.3289	0.3315	0.3340	0.3365	0.3389
1.0	0.3413	0.3438	0.3461	0.3485	0.3508	0.3513	0.3554	0.3577	0.3529	0.3621
1.1	0.3643	0.3665	0.3686	0.3708	0.3729	0.3749	0.3770	0.3790	0.3810	0.3830
1.2	0.3849	0.3869	0.3888	0.3907	0.3925	0.3944	0.3962	0.3980	0.3997	0.4015
1.3	0.4032	0.4049	0.4066	0.4082	0.4099	0.4115	0.4131	0.4147	0.4162	0.4177
1.4	0.4192	0.4207	0.4222	0.4236	0.4251	0.4265	0.4279	0.4292	0.4306	0.4319
1.5	0.4332	0.4345	0.4357	0.4370	0.4382	0.4394	0.4406	0.4418	0.4429	0.4441
1.6	0.4452	0.4463	0.4474	0.4484	0.4495	0.4505	0.4515	0.4525	0.4535	0.4545
1.7	0.4554	0.4564	0.4573	0.4582	0.4591	0.4599	0.4608	0.4616	0.4625	0.4633
1.8	0.4641	0.4649	0.4656	0.4664	0.4671	0.4678	0.4686	0.4693	0.4699	0.4706
1.9	0.4713	0.4719	0.4726	0.4732	0.4738	0.4744	0.4750	0.4756	0.4761	0.4767
2.0	0.4772	0.4778	0.4783	0.4788	0.4793	0.4798	0.4803	0.4808	0.4812	0.4817
2.1	0.4821	0.4826	0.4830	0.4834	0.4838	0.4842	0.4846	0.4850	0.4854	0.4857
2.2	0.4861	0.4864	0.4868	0.4871	0.4875	0.4878	0.4881	0.4884	0.4887	0.4890
2.3	0.4893	0.4896	0.4898	0.4901	0.4904	0.4906	0.4909	0.4911	0.4913	0.4916
2.4	0.4918	0.4920	0.4922	0.4925	0.4927	0.4929	0.4931	0.4932	0.4934	0.4936
2.5	0.4938	0.4940	0.4941	0.4943	0.4945	0.4946	0.4948	0.4949	0.4951	0.4952
2.6	0.4953	0.4955	0.4956	0.4957	0.4959	0.4960	0.4961	0.4962	0.4963	0.4964
2.7	0.4965	0.4966	0.4967	0.4968	0.4969	0.4970	0.4971	0.4972	0.4973	0.4974
2.8	0.4974	0.4975	0.4976	0.4977	0.4977	0.4978	0.4979	0.4979	0.4980	0.4981
2.9	0.4981	0.4982	0.4982	0.4983	0.4984	0.4984	0.4985	0.4985	0.4986	0.4986
3.0	0.4987	0.4987	0.4987	0.4988	0.4988	0.4989	0.4989	0.4989	0.4990	0.4990
3.1	0.4990	0.4991	0.4991	0.4991	0.4992	0.4992	0.4992	0.4992	0.4993	0.4993
3.2	0.4993	0.4993	0.4994	0.4994	0.4994	0.4994	0.4994	0.4995	0.4995	0.4995
3.3	0.4995	0.4995	0.4995	0.4996	0.4996	0.4996	0.4996	0.4996	0.4996	0.4997
3.4	0.4997	0.4997	0.4997	0.4997	0.4997	0.4997	0.4997	0.4997	0.4997	0.4998